UNIVERSITY OF CALIFORNIA, SAN DIEGO

GnRH induces miR-132 and miR-212 and reduces p250RhoGAP and SirT-1 in pituitary LbetaT2 Gonadotropes

A Thesis Submitted in partial satisfaction of the requirements
for the degree of Master of Science

in

Biology

by

Joseph Christopher Godoy

Committee in charge:

Professor Nicholas Webster, Chair
Professor Shelley Halpain, Co-Chair
Professor Chris Armour

2009

The Thesis of Joseph Christopher Godoy is approved and it is acceptable in quality and form for publication on microfilm and electronically:

_____

_____
Co-chair

_____
Chair

UNIVERSITY OF CALIFORNIA, SAN DIEGO

2009

DEDICATION

I would like to acknowledge the following past and present Webster lab members and thank them for their technical and moral support and guidance…

Lin Bo

Hao Zhang

Rie Tsutsumi

Shweta Sharma

Debin Lan

Devendra Mistry

Indrani Talukdar

Supriya Sen

Marine Nishimura

and

Nicholas Webster

EPIGRAPH

Basic Research is what I'm doing when
I don't know what I'm doing

Werner von Braun

TABLE OF CONTENTS

LIST OF ABREVIATIONS

AC	Adenylate Cyclase
Ac-p53	acetylated p53
BSA	bovine serum albumin
CREB	cAMP response element binding protein
FBS	fetal bovine serum
GAP	GTPase activating protein
GnRH	honadotropn heleasing hormone
GPCR	G-protein coupled receptor
HPG	hypothalamic-pituitary-gonadal axis
MEK	mitogen activated protein kinase
miRNA	micro RNA
miR-132/212	miR-132 and miR-212
MRE	miRNA recognition element
PLL	poly-L-lysine
TBST	tris-buffered saline with tween-20
Tx	treated, treatment
UCSC	University of California, Santa Cruz
UTR	untranslated Region

LIST OF SYMBOLS

*	p=0.01
**	p=0.001
***	p=0.0001
β	beta

LIST OF FIGURES AND TABLES

ACKNOWLEDGEMENTS

I must acknowledge Dr. Tadashi Yamamoto, University of Tokyo in exchange for his kind gift of p250RhoGAP polyclonal rabbit antibody, without which this research would not have been possible.

This Thesis, in full, is currently being prepared for submission for publication of the material. Godoy, Joseph; Lan, Debin; Webster, Nicholas JG.

ABSTRACT OF THE THESIS

GnRH induces miR-132 and miR-212 and reduces p250RhoGAP and SirT-1 in pituitary LbetaT2 Gonadotropes

by

Joseph Christopher Godoy

Master of Science in Biology

University of California, San Diego, 2009

Professor Nicholas JG Webster, Chair

Professor Shelley Halpain, Co-Chair

Gonadotropin releasing hormone (GnRH) is vital to the proper pituitary gonadotrope function as it regulates LH and FSH synthesis and secretion. GnRH causes cell-cycle arrest in pituitary LbetaT2 gonadotrophs, leading to apoptosis. Microarray and q-PCR analyses show that the mouse EST,

AK006051, encoding two intronic micro-RNAs, miR-132 and miR-212, is highly induced under GnRH treatment. As miR-132/212 have been linked to neuronal development, we hypothesized that these miRNAs might be linked to cell-cycle arrest in LbetaT2 gonadotrophs. GnRH treatment for increasing times causes a dose-dependent increase in AK006051 promoter activity and a concomitant increase in miR-132/212 expression which is abolished by pretreatment with the adenylate cyclase inhibitor SQ22536 and the MEK inhibitor U0126. Marked increases in both the number and morphology of neurites protruding from LbetaT2 cells are observed after 24h of GnRH treatment. As well, GnRH causes a pulse frequency-dependent increase in AK006051. GnRH inhibits p250RhoGAP expression through a miR-132/212 response element within the 3' UTR of p250RhoGAP. Knockdown of p250RhoGAP by siRNA induces the same morphology observed with GnRH treatment. Since p250RhoGAP stimulates proliferation in fibroblasts and suppresses neurite outgrowth in neurons, our findings suggest that miR-132/212 induction by GnRH is required for cell cycle arrest. We also suggest that apoptosis is due to degradation of SirT-1, another miR-132/212 target, leading to unchecked activation of p53. In conclusion, these data suggest a mechanism by which gonadotrophs synchronize their responses to GnRH leading to coordinated LH and FSH secretion by modulating synaptic-like contacts between gonadotrophs thereby regulating reproductive function.

INTRODUCTION

The integration and precise coordination of hormones across the hypothalamic-pituitary-gonadal axis (HPG) is essential for sexual maturation and reproductive function in mammals. The hypothalamic decapeptide gonadotropin releasing hormone (GnRH) stimulates the synthesis and secretion of pituitary gonadotrophins Leuteinizing hormone (LH) and follicle stimulating hormone (FSH) through signaling via the GnRH receptor (GnRH-R) expressed by pituitary gonadotrophs (1,2). LH and FSH then go on to regulate most of the reproductive functions of both sexes through the production of gonadal steroids and regulation of gametogenic and hormonal functions.

The GnRH-R, a member of the G protein-coupled receptor (GCPR) family, is associated with Gs, Gi, and Gq/11 (3). Among the plethora of intracellular signaling cascades upon GnRH-R activation at the cell surface, Gs activates adenylate cyclase (AC), which in turn induces cAMP production. This leads to activation of protein kinase A (PKA) which phosphorylates the activation domain of the transcription factor cAMP response element binding protein (CREB) (4-7). CREB activation is involved in many neuronal processes including neuronal survival, proliferation, differentiation, morphogenesis, and plasticity as well as addiction and circadian rhythms (8). The other arm of G-protein signaling via Gq/11 activates phospholipase C leading to formation of inositol 1,4,5-triphosphate (IP3) and diacylglycerol (DAG). Release of intracellular calcium and

activation of protein kinsase C then follow, which results in the activation of ERK, p38, and JNK as well as many other transcription factors (2, 9-10).

In animals, GnRH is released in a pulsatile fashion from the hypothalamus into the hypohyseal portal system. Such episodic exposure to GnRH is essential for gonadotrope function and causes pulsatile release of LH and FSH into the circulation (11). The pulse amplitude and frequency of GnRH release greatly increases prior to ovulation and is essential for inducing the requisite LH surge. LβT2 cells are an immortalized cell line originating from mouse gonadotrophs and driven by the SV40 T antigen (12, 13). They are also sensitive to GnRH pulses and respond by altering gene expression and LH and FSH secretion accordingly (12, 13). *In vitro* studies of pituitary gonadotrophs usually involve the tonic treatment of GnRH. Our lab and others have shown that this causes G1/G0 arrest and apoptosis in LβT2 cells (14, 15). GnRH stimulation also mediates plasticity in LβT2 cells and pituitary gonadotrophs *in vivo* (16).

Although there have been many discoveries that shed light on the complex network of signaling pathways leading to transcriptional regulation in the HPG axis, not much is known about post-transcriptional regulation, specifically the role of microRNAs (miRNA). MicroRNAs are single-stranded RNA molecules of about 21-23nt that regulate gene expression post-transcriptionally by targeting the 3' untranslated region (3'UTR) of specific mRNAs (17). MiRNAs are generally located within the intronic sequences of genes and are transcribed by

RNA polymerase II (18). Primary miRNA transcripts (pri-miRNA) form a stem-loop structure for each miRNA encoded by the transcript (19). Each stem-loop is then cleaved by Drosha, an RNAse III, to form the pre-miRNA, which is subsequently transferred from the nucleus to the cytoplasm by Exportin 5 (20, 21). The pre-miRNA then associates with and is cleaved by Dicer of the RISC complex into functional a miRNA (22, 23). Mature miRNA are partially complementary to a sequence located in the 3'UTR of mRNA, known as the miRNA recognition element (MRE) (22). The first seven nucleotides of the miRNA after the initial adenine are called the seed sequence. This specifies targeting while the remaining sequence is thought to stabilize the miRNA-target complex (22, 23). Annealing of miRNA to its target sequences can inhibit translation either by blocking protein translation machinery or by sequestering the mRNA transcript away from ribosomal interaction. MiRNA targeting can also trigger mRNA degradation in a similar process to RNA interference. In mammals the specificity of miRNA binding to its cognate MREs and the ultimate fate of the target mRNAs are still being elucidated (24).

The study of miRNAs has unlocked a great deal of understanding of the role of post-transcriptional regulation in development, differentiation, and normal functioning of tissues (25-27). Yet, the study of miRNAs in the reproductive system is just beginning and there is very little published data on miRNA activity in gonadotropes (28). Much of the GnRH response in both gonadotrophs and LβT2 cells is mediated via the regulation of gene transcription. We hypothesize

that the GnRH response may be further regulated by miRNAs at the post-transcriptional level. If GnRH down regulates the transcription of certain genes, the miRNAs will act in concert and reduce translation of the existing transcripts of those genes, thereby generating a swift GnRH response. Here we wish to determine the mechanisms regulating these events following GnRH stimulation in LβT2 gonadotrophs and hope to shed light on the normal control of pituitary gonadotroph function and its synchrony in the HPG axis. We show that GnRH induces the gene encoding miR-132/212 in a pulse frequency-dependent manner. We also confirm that p250RhoGAP and SirT-1 are miR-132/212 targets in LbetaT2 cells. Our data suggests that miR-132/212 may play a vital role in the coordination of the cyclic control of gonadotropin release and ultimately reproductive function.

MATERIALS AND METHODS

Cell culture and Stimulation.

LβT2 cells, a gift from Dr. Pam Mellon (UCSD), at passages 13-19 were cultured in monolayers with DMEM containing 10 % FBS, penicillin/streptomycin, and Gluta-max (Gibco) in a humidified 10 % CO2 atmosphere at 37˚C. Cells were plated at $1x10^6$ cells/ml in triplicate in 12- and 6-well plates or 6-cm dishes coated with poly-L-lysine(Sigma) or Matrigel® (1:150 dilution, BD Biosciences). After 24 hours, cells were starved in DMEM containing 0.5% FBS, penicillin/streptomycin, and Gluta-max for an additional 24 hours. Cells were then stimulated with 10nM GnRH for .5-48h in starvation media. Inhibitors of MEK and AC (U0126: 5μM; PD98059: 5μM; SQ22536, 100μM; Calbiochem) were added 1h before the 10nM GnRH stimulation. For pulse frequency experiments, cells were washed with starving media supplemented with 2ng/ml activin (Sigma) every half hour and pulse treated with starvation media containing 10nM GnRH for two minutes every half hour or two hours. Apoptosis/Necrosis was detected by enhanced Cy3-conjugated Anexin V (Enzo Life Sciences) staining on live cells.

MicroArray and Quantitative PCR.

For the microarray study, the mRNA was isolated from total RNA using the ribosomal RNA reduction kit (Invitrogen) and subsequently labeled using the NCODE labeling kit. RNA from unstimulated cells was labeled with Cy3 and RNA from GnRH stimulated cells with Cy5. Labeled probes were hybridized to NCODE arrays in duplicate. For qPCR, total RNA was purified with RNA-Bee (Tel-test) according to manufacturer's protocol and first strand cDNA synthesis was done using the cDNA Reverse Transcription Kit (Applied Biosystems). Samples for qPCR were run in 20 μL triplicate reactions on a MJ Research Chromo4 instrument using iTaq SYBR Green Master Mix (Bio-Rad). Sequence-specific primers for AK006051, p250RhoGAP, SirT-1, Beta-actin, and GAPDH were designed using the Universal Probe Library Assay Design Center (Roche). Mature miRNA expression was quantitated using Taqman Micro-RNA Assays (Applied Biosystems) for miR-132 and miR-212 and normalized to miR-30c expression, which does not change with GnRH treatment (Table 1). Gene expression levels were calculated after normalization to the housekeeping genes, GAPDH and/or Beta-actin, using the $\Delta\Delta$Ct method and expressed as fold mRNA expression levels with respect to non-treated cells. Error bars are SEM.

Western Blot.

LβT2 cells were washed twice with cold PBS and lysed with 3X RIPA buffer (Stratagen). Lysates were sonicated and then centrifuged for 20 minutes at 14,000 rpm, 4°C. Total protein was quantitated from the supernatants using Bio-Rad's DC Protein Assay, and 25-35ng protein per sample was loaded with LDS loading buffer (Invitrogen) onto 4-12% gradient Bis-Tris Criterion gels (Bio-Rad) prior to electrophoresis The following polyclonal primary antibodies were used overnight at 4C in TBST, 5% BSA, .and 02% sodium azide: anti-p250RhoGAP (Dr. Tadashi Yamamoto, University of Tokyo), SirT-1 (Santa Cruz), Beta-tubulin (Santa Cruz), p44/p42 MAPK and acetylated-p53 (Cell Signaling) .

Transfection, Knock-Down, and Reporter Assays.

LβT2 cells were transfected by electroporation using the Microporator (Digital Bio Technology) using parameters optimized according to manufacturer's protocol with Pre-mir-132, Pre-miR control, pre-designed siRNA against p250RhoGAP, or scrambled siRNA control (Ambion). A pair of locked nucleic acid (LNA) oligos was designed against miR-132/212 with the following complimentary sequences: CTG(T/G)AGACTGTTA. SirT-1 siRNA was from Santa Cruz Biotechnology.

A luciferase reporter plasmid for the AK006051 promoter region, pAK-1.3-luc, was constructed using the region 1.3kb upstream of the AK006051 transcriptional start site, which was amplified using PfuUltra (Stratagene). The AK006051 promoter region was inserted into the pAP1-luc reporter vector (Clontech) after removal of the AP1 promoter region by restriction digest. A control reporter, pAK-.2-1.3-luc, was also constructed in which the first 200bp upstream of the transcriptional start site containing the TATA box was deleted.

One copy of the miR-132 and miR-212 target site in the 3'UTR of p250RhoGAP was cloned into the pIS vector containing a MCS downstream of Firefly Luciferase ORF as described (Lewis and Bartel). Two mutants were also constructed in which the UTR region complementary to either the 5' or 3' region of miR-132/212. Inserts were constructed by Klenow fill-in with Sac I, Spe I, and Xba I restriction sites. Luciferase plasmids were co-transfected with concentrations of 500ng per $5x10^5$ cells along with 25ng TK-lacz. Luciferase and beta-galactosidase activity were measured by the Veritas Microplate Luminometer (Turner BioSystems) using luciferin (Sigma) and Galacto-light assay kit (Applied Biosystems). Data is fold luciferase activity in GnRH-stimulated cells normalized to beta-galactosidase activity versus non-treated cells. Error bars are SEM.

RESULTS

LβT2 cells undergo morphological changes, apoptosis, and altered microRNA expression under tonic GnRH treatment.

Previous studies have shown the antiproliferative and apoptotic effects of GnRH treatments longer than 12 hours (14,15). Although serum starvation alone causes the appearance of small floating cells, indicative of apoptosis, we see here that not only does GnRH stimulation increase the appearance of cell death there are also marked morphological changes induced by prolonged tonic exposure to GnRH (Figure 1). A densely packed monolayer of cells is reduced significantly with an increase in the number of floating cells and blebbing on surviving cells. Individual surviving cells take on different shapes from squamosal to more elongated and form multiple outgrowths. Projections extend from cell to cell at 18 hours of treatment. By 48 hours the surviving cells have taken on a completely different morphology and formed what looks like interconnected networks.

Extracellular matrix is required for differentiation and the support of neurite outgrowth by neurons and other cells *in vivo* and *in vitro* (31-38). As reconstituted basement membrane affects LH and FSH secretion in primary cultures of rat gonadotrophs, and gonadotrophs may be capable of matrix remodeling via activated MMP2 and MMP9 (36, 37), we wanted to see if it would

also facilitate outgrowth formation and the development of a more elaborate network of “neurites” in GnRH-stimulated LβT2 cells. Although gonadotrophs strictly are not neurons, we will refer to the outgrowths projecting from LβT2 cells as neurites for simplicity. Matrigel is the commercially available reconstituted basement membrane purified from the Engelbreth-Holm-Swarm mouse sarcoma that consists mainly of laminin, collagen IV, and enactin. Pre-coating dishes with poly-L-lysine and Matrigel induces differentiation and promotes basal level of neurite outgrowth in LβT2 cells (Figure 2). However, GnRH-treated cells exhibit a robust increase in the occurrence, length, and elaboration of neurites among cells.

In order to quantify the apparent apoptosis induced by GnRH, we stained cells with Anexin V. Consistent with other’s findings (14), GnRH treatment increases apoptosis/necrosis of cells to 52%(+/-12%) versus 18% (+/- 5%) in non-treated cells (Figure 3). In order to elucidate the mechanisms by which these morphological and apoptotic changes occur and at the same time make a connection between GnRH signaling in gonadotrophs with post-transcriptional regulation by miRNA, a microarray was performed on the miRNA from LβT2 cells at 24 hours following GnRH treatment (Figure 4, Table 1). Out of about 280 mouse miRNAs that were spotted on the NCODE chip, only 85 were detected in LβT2 cells, most of which were not significantly up or down regulated. Among the most highly upregulated miRNAs, miR-212 expression was induced 41-fold, and miR-132 was induced 10-fold. This was verified by qPCR for the mature

forms of miR-132/212 (Figure 5). We selected miR-30c as an internal control for LβT2 cells based on the microarray data showing that its expression is unchanged by GnRH.

miR-132 and miR-212 are coordinately regulated and localize to the same chromosomal region

MiR-132/212 were traced to the first intron of the non-coding mouse EST AK006051 using the UCSC genome browser (Figure 6). The entire intron is located within a CpG island and both miR-132/212 have CRE consensus sequences directly upstream indicating that miR-132/212 may be highly regulated (39). Interestingly, their seed sequences differ by only a single nucleotide and thus likely have the same target mRNAs. QPCR analysis shows robust induction of AK006051 as early as 30 minutes under GnRH treatment (Figure 7). The induction is reduced at 24 hours, although it remains significantly upregulated even at 48 hours.

In addition to miR-132/212 being highly conserved among vertebrates, it seems the promoter region of AK006051 is also highly conserved according to the UCSC genome browser. This may imply that other signaling pathways besides those leading to CREB activation may modulate miR-132/212 espression. In order to elucidate signaling events upstream of AK006051

induction, we pre-treated cells with the adenylate cyclase inhibitor SQ22536 or the MEK inhibitors U-0126 or PD89059. Pre-treatment with SQ22536 reduces the GnRH-induced increase in AK006051 mRNA, confirming cAMP-mediated miR-132/212 induction (Figure 7). Interestingly, Erk1/2 is also important for GnRH-induced AK006051 expression in LβT2 cells. In order to investigate the promoter activity of AK006051, we constructed a reporter plasmid dubbed pAK-1.3k-luc by cloning 1.3kb upstream of the transcriptional start site and inserting it into the pAP1 luciferase vector after removing the AP1 promoter (Figure 8A). We also made a control vector, pAK-.2-1.3-luc, in which 200bp upstream of the transcriptional start site, including the TATA box, was deleted from the insert. Following GnRH treatment in transfected cells, luciferase activity was robustly increased up to 45-fold as early as 4 hours, 14-fold at 24 hours and 5-fold at 48 hours over basal levels in non-stimulated cells (Figure 8B). Therefore the promoter region alone is sufficient for the strong induction of AK006051 transcription.

Since pulsatile GnRH stimulation is necessary for proper gonadotroph function and LβT2 cells exhibit pulse-sensitivity with respect to LH and FSH expression and secretion, we wanted to investigate whether AK006051 is also differentially regulated by GnRH pulse frequency. In mice GnRH pulse frequency ranges from 30 minutes to 120 minutes, so we stimulated cells with GnRH using the same intervals for 2 minutes each for 6 hours. For both treatment conditions and non-treated, the media was changed to fresh starving media every 30

minutes. Our data shows that AK006051 mRNA is differentially up regulated by GnRH pulse frequency (Figure 9). While there is significant induction with the low frequency pulses, the high frequency pulses further induce AK006051 expression by more than double.

Degradation of p250RhoGAP and SirT-1 are required for GnRH-induced neurite outgrowth, cell cycle arrest, and apoptosis.

Among the hundreds of predicted miR-132/212 targets is p250RhoGAP, also known as RICS, Grit, and p200 RhoGAP (Table 2, 3). Rho GTPases are a subfamily of small GTPases (21-25kDa). The Rho GTPases RhoA, Rac1, and Cdc42 are intracellular binary molecular switches that regulate actin cytoskeleton rearrangements including stress fiber, lamellapodia, and filopodia formation as well as transcriptional activation, cell growth, cell survival, and vesicle trafficking. Like other G-proteins the Rho GTPases cycle between active and inactive forms depending on their interaction among three regulators (40-43). When Guanine nucleotide exchange factors (GEF) exchange GDP bound by the inactive Rho GTPase for GTP, the Rho GTPase becomes active. RhoGAPs are a GTPase activating proteins (GAP) that highly induce a Rho protein's GTPase activity, thereby deactivating it. Guanine nucleotide dissociation inhibitors (GDI) stabilize the Rho GTPase-GDP bond, also deactivating it. (40-43). Also, it has been

shown that p250RhoGAP can promote proliferation by interacting with another GAP, RasGAP, and as a result allowing ERK activation (44).

Another likely miR-132/212 target is the Silent Information Regulator SirT-1, a NAD-dependent histone deacetylase that regulates apoptosis in response to DNA damage and oxidative stress (45, 46). It acts anti-apoptotically by deacetylating one of its non-histone targets, the tumor suppressor protein p53 (45). This negatively regulates p53-mediated transcription, thus preventing cellular senescence and apoptosis induced by DNA damage and stress.

A previous study has confirmed p250RhoGAP as both a miR-132/212 target and a regulator of dendritic plasticity in hippocampal neurons (48). However, SirT-1 has so far only been shown to be targeted by miR-34a, which is linked to proliferation, apoptosis, and senescence (49-50). In LβT2 cells both mRNA and protein levels of p250RhoGAP and SirT-1 are reduced under GnRH stimulation (Figure 10). In order to test whether the 3'UTR of p250RhoGAP is responsible for the degradation of p250RhoGAP, we constructed a reporter plasmid according to previously established methods for studying miRNAs (51). A modified pGL3 control vector (Promega), pIS-0 is a firefly luciferase vector in which a short multiple cloning site (MCS) was inserted immediately downstream from the stop codon. Our reporter plasmid, pIS-U, was constructed by cloning the (MRE) of p250GAP into the MCS of the pIS luciferase plasmid (Figure 11A) (51). We also constructed the mutants pIS-5, which has a mutation in the 5' end

complementary to the miRNA, and pIS-3, which has a mutation in the 3' end. After 24 hours of GnRH stimulation, there is no change in luciferase activity in the two mutants, suggesting that degradation may require precise very annealing of the miRNA to its target (Figure 11B). However, luciferase activity is reduced by half in pIS-U transfected cells, confirming that the MRE of p250RhoGAP is important for mediating down regulation of mRNA under GnRH stimulation.

In order to confirm that miR-132/212 are responsible for the degradation of p250RhoGAP and SirT-1, we co-transfected cells with pre-miR132 and saw a significant decrease in mRNA after 48 hours (Figure 12A). We also transfected cells with a locked nucleic acid (LNA) complimentary to the seed sequences of miR132/212 or scrambled control for 48 hours prior to 24 hours of GnRH treatment. This abolished the GnRH-induced reduction in p250RhoGAP and SirT-1 mRNA (Figure 12B).

In order to elucidate the functional effects of p250RhoGAP degradation, we knocked down p250RhoGAP by siRNA (Figure 13). Negative control scrambled siRNA-transfected cells exhibited neurite outgrowth similar to that seen in non-transfected cells with and without GnRH stimulation (Figure 14). Knockdown of p250RhoGAP alone was sufficient to increase the number and length of neurite outgrowths and induce the branching and network pattern seen in GnRH-stimulated cells. Stimulation of siRNA-transfected cells with GnRH did

not significantly change morphology any further than siRNA alone indicating that p250RhoGAP is the main regulator of plasticity in gonadotrophs.

In order to determine the role of SirT-1 in GnRH-induced apoptosis, we knocked down SirT-1 by siRNA (Figure 15). SirT-1 degradation by siRNA and GnRH stimulation corresponds to an increase in acetylated p53 (Ac-p53). P53 is a tumor suppressing transcription factor that inhibits proliferation and induces apoptosis in response to DNA damage and oxidative stress (52, 53). Acetylation of p53 protects it from ubiquitination by Mdm2 and is required for binding to the promoter of p21 (54, 55). Consistent with our previous data (14), GnRH stimulation increases the direct downstream targets of p53, p21 and PUMA. Thus, the degradation of SirT-1 is likely to be responsible for the antiproliferative and apoptotic effects of GnRH.

DISCUSSION

In this study, we establish that GnRH inhibits p250RhoGAP and SirT-1 expression by inducing mir-132/212 in LβT2 cells. Microarray anaylsis identified 85 differentially expressed miRNA transcripts in GnRH stimulated LβT2 cells suggesting the likelihood that post-transcriptional regulation via miRNA is an integral factor in the GnRH response. The qPCR results for AK006051 and mature miR132/212 indicate that miR-132/212 were rapidly upregulated by GnRH and that their mature forms remain elevated even after the decline of AK006051 induction. This indicates prolonged activity of miR-132/212 which may play a critical role in mediating the GnRH response. We have shown that the highly robust induction of AK006051 by GnRH is likely due to adenylate cyclase activation and the cAMP signaling cascade, which coincides with previous studies demonstrating the cAMP-dependent increase in miR-132/212 in several other cell lines, primary cultures, and tissues. As well, miR-132/212 has been shown to be under the direct control of the CREB response elements located immediately upstream of the miR-132/212 sequences. Our AK006051 promoter assay indicates that the AK006051 promoter may also play a significant role in miR-132/212 induction.

In order to determine the most likely proteins regulated by miR-132/212, we compared the lists generated by TargetScan, miRanda, and miRacle of predicted targets having putative miR-132/212 recognition sites. From there we

chose to study p250RhoGAP and SirT-1 as they have been identified as targets in other tissues and relevant to the regulation of morphology, proliferation, and apoptosis. Pre-miR-132/212 alone reduces both transcripts, and anti-miR-132/212 rescues GnRH-induced degradation of p250RhoGAP and SirT-1. Our data indicate that both p250RhoGAP and Sirt-1 are indeed regulated post-transcriptionally by the GnRH induction of miR-132/212 in LβT2 cells.

Our data also indicate the likelihood that cell cycle arrest and/or apoptosis is mediated via p53 activation that is left unchecked following SirT-1 degradation. We believe this occurrence is only significant under tonic stimulation of GnRH in static culture. In the normal functioning pituitary, it is unlikely that gonadotropes commit mass suicide in response to increased GnRH pulse frequency at every cycle. As well, there is no documented histological analysis of the adenohypophysis indicating any detectable levels of cell death in normal animals. Further, SirT-1 female knockout mice do not exhibit detrimental decreases in fertility (56, 57).

Others have demonstrated the importance of miR-132/212 in ovaries (58). We show that miR-132/212 are differentially modulated by GnRH pulse frequency. While others have also shown that GnRH induces neurite outgrowth in LβT2 cells as well as *in situ* locomotion in *ex vivo* gonadotropes within the pituitary, they conclude that individual gonadotropes are migrating to the portal vasculature and forming processes from which they secrete LH and FSH (16).

However, they have studied single cells or cultures in very low density. Can it be that gonadotrophs are searching for other gonadotrophs? Also, if cells are already forming projections from which they can secrete LH and FSH, do they really need to move closer to the vascular epithelium to do so? We suggest instead that under high frequency GnRH stimulation pituitary gonadotrophs establish a communication network in order to coordinate the LH and FSH surge. Any observed movement likely occurs in order for individual cells to quickly find each other. We observe a tendency for LβT2 cells to form rafts or clumps of cells instead of a clearly defined monolayer in culture. Further, a much more elaborate meshwork of neurites is observed between two larger masses of cells than between two smaller masses of cells. We also believe that gonadotrophs do enter G0 in order to commit most of their energy expenditures to neurite outgrowth and any amount of locomotion. We believe cell cycle arrest to be mediated to a greater extent by p250RhoGAP degradation than by SirT-1 degradation as p250RhoGAP is only associated with proliferation and cell cycle and not apoptosis (48).

We propose that low frequency stimulation primes gonadotrophs such that high frequency stimulation quickly induces neurite outgrowth. The subsequent miR-132/212-mediated p20RhoGAP suppression will then allow both Rac1 and Cdc42 to remain active (48, 59-61). Rac1 and Cdc42 would then go on to mediate the morphological changes we and others have observed, primarily the induction of process formation and branching (59-63) by individual gonadotrophs

in order to locate and contact each other. Rac1 and Cdc42 might further mediate cell-to-cell communication among gonadotrophs by establishing and maintaining dendritic spines (64, 65), although it is difficult to speculate as to how gonadotrophs would actually communicate once such networks are established. We do, however, maintain that the observed networks of processes among LβT2 cells and those that may form among gonadotrophs *in vivo* likely serve to coordinate the LH/FSH surge required for ovulation.

In conclusion, our studies have demonstrated the likelihood of a functional role that miR-132/212 may play in the GnRH response by LβT2 cells, as well as the possibility that miR-132/212 may have an even greater role in the global regulation of reproduction.

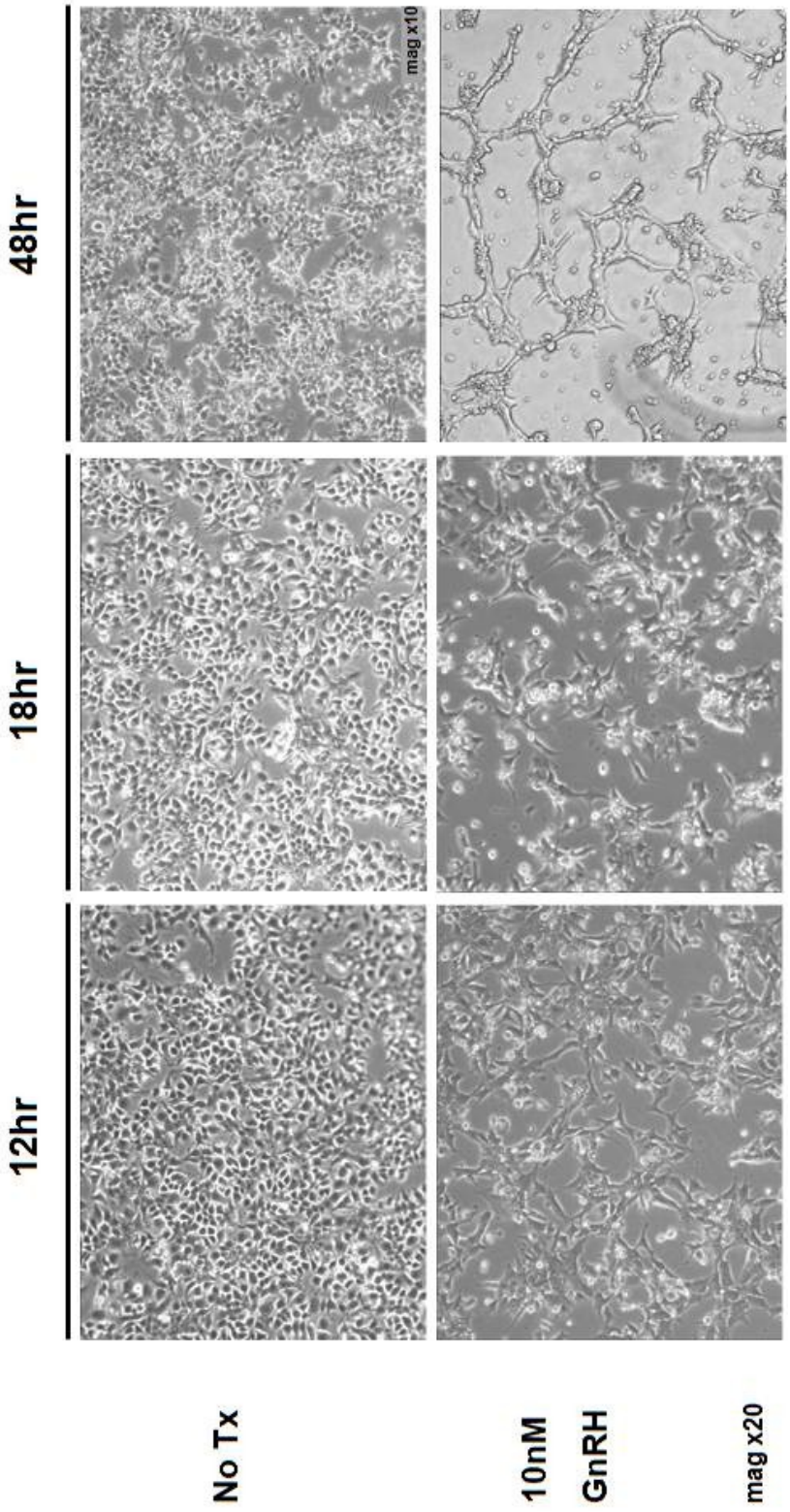

Figure 1. GnRH induces neurite outgrowth and apoptosis in LβT-2 cells.
LβT-2 cells were cultured in monolayers overnight in DMEM containing 10% FBS, antibiotics, and Gluta-Max (Sigma). Cells were then washed once with PBS and starved for 24 hours in DMEM containing 0.5% FBS, antibiotics, and Gluta-Max. Cells were then treated or non-treated by replacing the media with fresh starving media containing 10nM GnRH or not for 12, 18, and 24 hours.

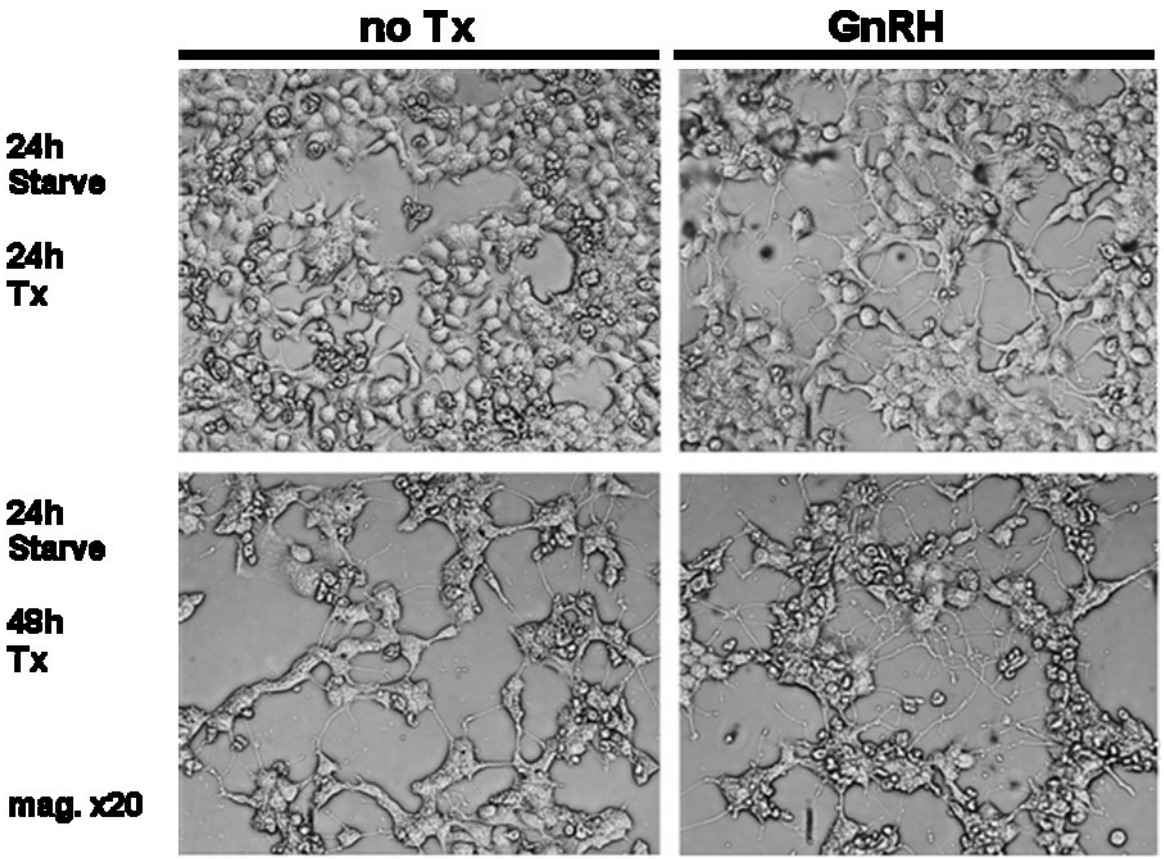

Figure 2. Reconstituted basement membrane promotes elaborate neurite outgrowth.
Dishes were coated with poly-L-lysine and Matrigel (1:200 dilution). Cells were seeded and cultured in mololayers for 24 hours followed by 24 hours starvation. Time indicates duration of GnRH stimulation after initial starvation.

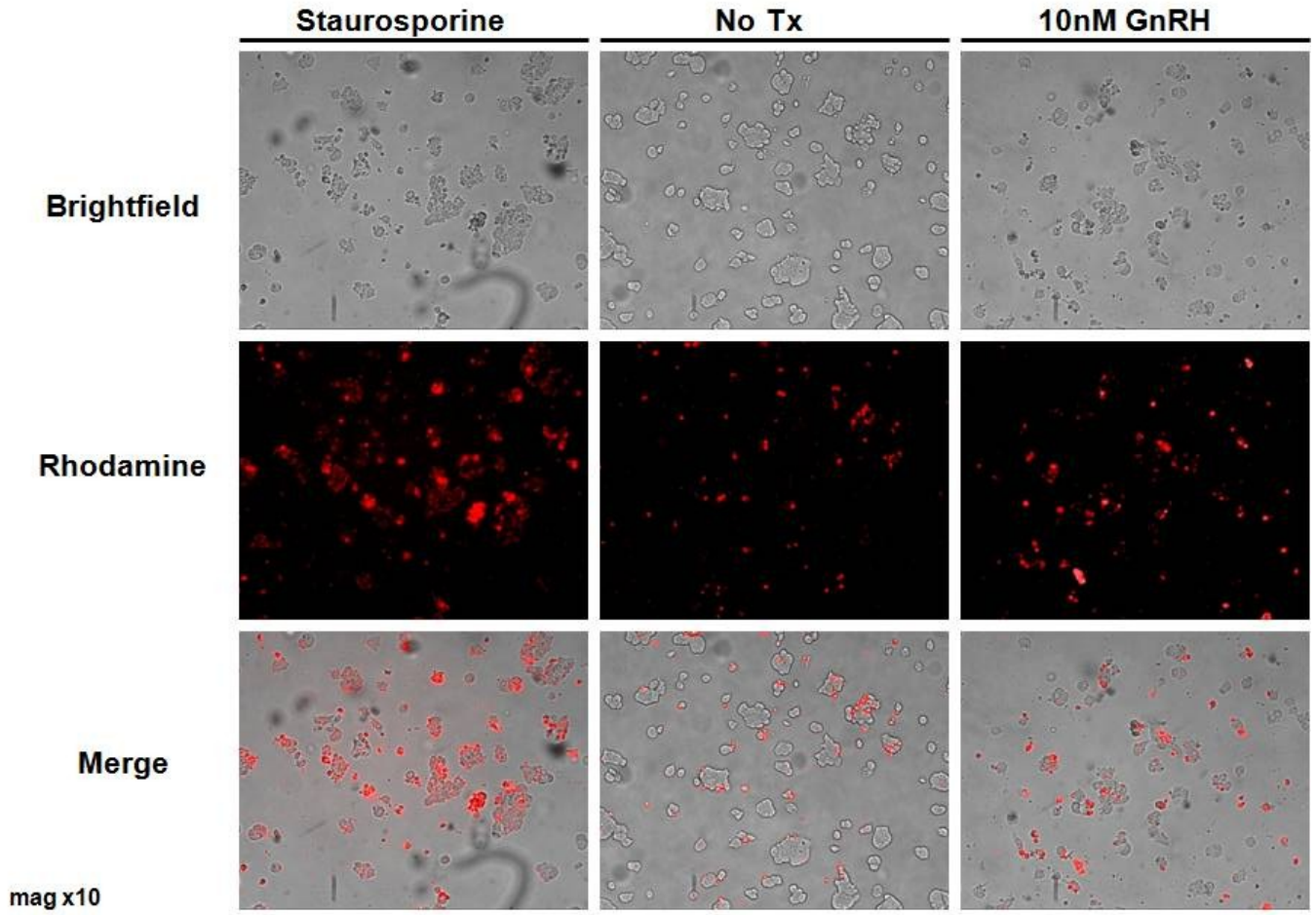

Figure 3. GnRH induces Apoptosis.
$1x10^6$ cells per well were cultured in uncoated 6-well plates for 24 hours prior to an additional 24 hours of starvation. Media was then replaced with fresh starvation media with or without 10nM GnRH. The apoptosis inducer straurosporine was added to the media 4 hours prior to Anexin V staining on live cells. Apoptosis/necrosis occurred in 18% ±5% of non-treated (No Tx) cells and 52% ±12%.

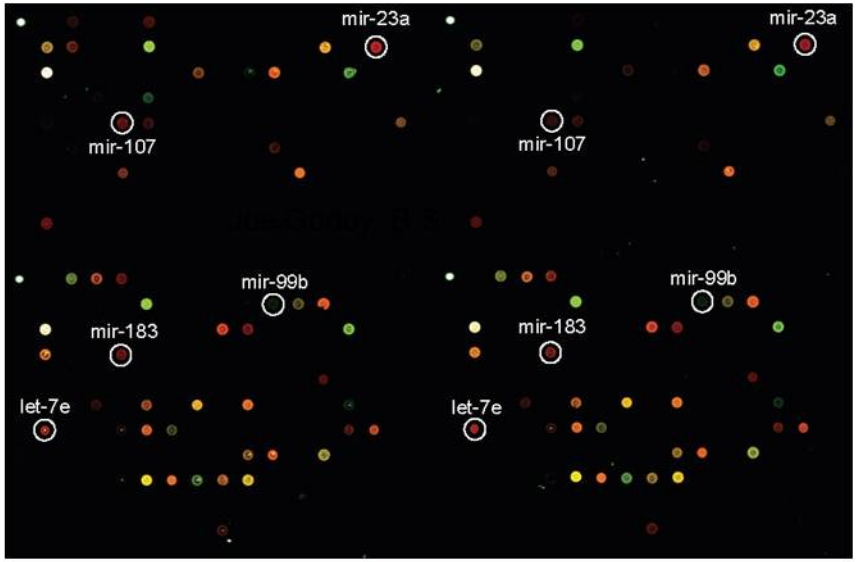

NCODE arrays ~280 mouse miRNAs

Figure 4. MicroArray Chip of miRNA expression in LβT2 cells.
(A) Cells were cultured and treated with 100nM GnRH for 24 hours prior to harvesting. Eighty five miRNs were detected (colored spots). (B) Of the ~280 miRNA probes on the NCODE chip, 85 were detectable over background. Data shows expression relative to baseline. Only the miRNAs at the ends of the graph show significant changes in expression.

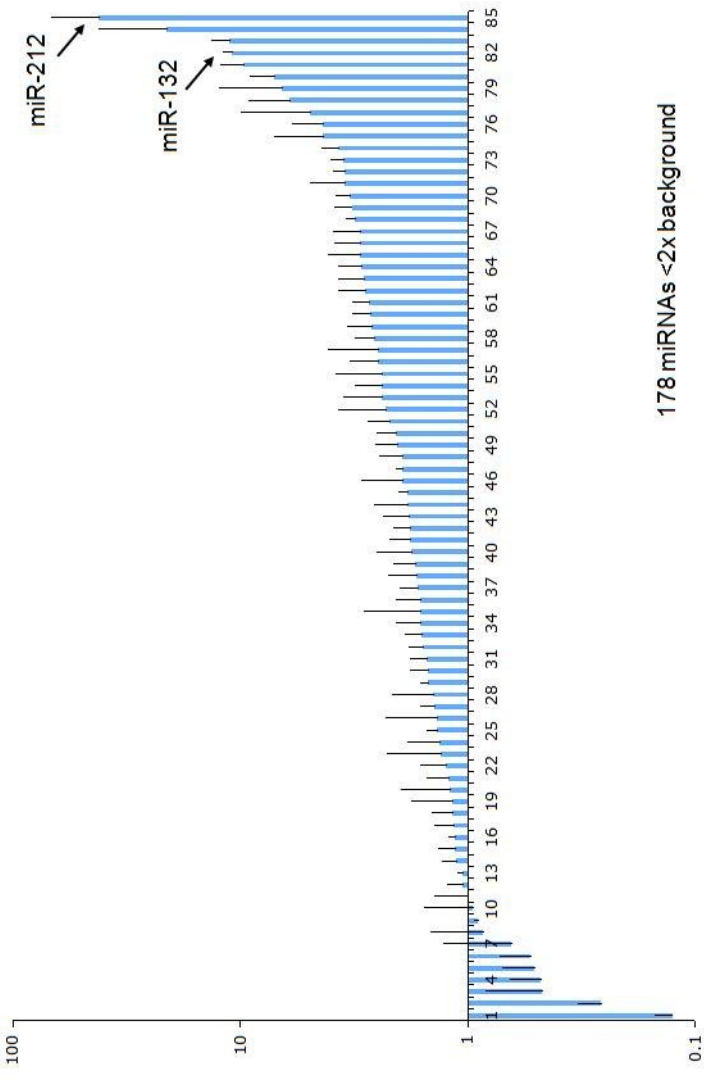

Figure 4, Continued. MicroArray Chip of miRNA expression in LβT2 cells.
(A) Cells were cultured and treated with 100nM GnRH for 24 hours prior to harvesting. Eighty five miRNs were detected (colored spots). (B) Of the ~280 miRNA probes on the NCODE chip, 85 were detectable over background. Data shows expression relative to baseline. Only the miRNAs at the ends of the graph show significant changes in expression.

Table 1 LβT2 cells express 85 miRNAs. miRNA Expression Profiling in LβT2 Cells in Response to 24h GnRH

miRNA ID	Combined Mean ratios 635/532	SD mean ratios	Z-test
01: J-04 2510_mmu_miR_99b	0.1265	0.02514624	3.1788E-05
01: J-02 2514_mmu_miR_125b	0.2605	0.07135592	2.1881E-01
03: F-08 2597_mmu_miR_19b	0.47175	0.37029211	0.0000E+00
01: F-17 C003_Ncode_Control	0.47775	0.18035405	6.9879E-04
02: J-18 2530_mmu_miR_140*	0.51	0.20334699	2.6351E-03
01: F-18 C003_Ncode_Control	0.52775	0.20909228	1.0022E-05
02: N-18 2531_mmu_miR_141	0.64275	0.64403125	6.2679E-06
02: B-09 2666_mmu_miR_210	0.849	0.61639435	2.2687E-04
01: B-04 2508_mmu_miR_30b	0.90175	0.04723258	3.3077E-05
03: J-24 2566_mmu_miR_203	0.943	0.63209862	1.8179E-01
03: N-06 2603_mmu_miR_200a	1.00275	0.40781481	1.0130E-02
03: B-12 2588_mmu_miR_301	1.04725	0.19170355	0.0000E+00
03: J-08 2598_mmu_miR_30c	**1.04825**	0.07847452	6.2205E-01
03: N-10 2595_mmu_miR_106b	1.128	0.19172376	6.9808E-09
03: N-02 2611_mmu_miR_16	1.1375	0.2163739	0.0000E+00
03: J-10 2594_mmu_miR_106a	1.1385	0.09210682	2.2221E-03
01: J-18 C004_Ncode_Control	1.149	0.27047859	1.9980E-01
01: J-17 C004_Ncode_Control	1.1585	0.30061992	1.2568E-13
04: B-24 2612_mmu_miR_18	1.161	0.62277711	6.7867E-02
02: F-19 2647_mmu_miR_342	1.193	0.78544892	2.4144E-03
01: F-02 2513_mmu_miR_125a	1.2165	0.32410441	6.2417E-01
01: J-07 2624_mmu_miR_93	1.246	0.38373949	4.4409E-16
01: N-17 C005_Ncode_Control	1.30725	0.9824352	2.9166E-01
01: F-01 2635_mmu_miR_325	1.3225	0.5415524	2.5436E-10
02: N-06 2555_mmu_miR_24	1.35775	0.17236081	2.0741E-02
01: N-18 C005_Ncode_Control	1.37125	0.95703165	6.2312E-01
02: J-13 2660_mmu_miR_25	1.39225	0.23141215	0.0000E+00
01: B-14 2557_mmu_miR_191	1.4225	0.76446648	4.3785E-01
03: J-02 2610_mmu_miR_15a	1.4855	0.13949074	2.8978E-04
01: F-09 2619_mmu_miR_29a	1.4905	0.32334966	8.5688E-01
01: N-05 2629_mmu_miR_103	1.5165	0.29409806	1.9241E-02
03: N-08 2599_mmu_miR_30d	1.5725	0.26681642	2.7057E-01
02: F-04 2557_mmu_miR_191	1.5805	0.32147628	2.3365E-01
01: F-11 2665_mmu_miR_200c	1.60675	0.49027841	3.8044E-06
04: N-24 2615_mmu_miR_22	1.61275	1.27905991	7.8576E-02
02: B-24 2516_mmu_miR_126_3p	1.617	0.47990485	6.2026E-02
01: J-10 2635_mmu_miR_325	1.665	0.36072242	2.3966E-05
01: F-13 1538_mut1_mir_200c	1.6735	0.58322351	1.1502E-04
02: N-02 2563_mmu_miR_200b	1.697	0.45573018	3.0447E-04
01: J-06 2506_mmu_miR_30a_5p	1.774	0.7672644	2.3050E-03
02: N-24 2519_mmu_miR_130a	1.79425	0.43829547	9.8924E-01
02: B-02 2560_mmu_miR_195	1.8015	0.34044334	4.4402E-04
02: J-19 2648_mmu_miR_344	1.815	0.55432662	2.8485E-05
03: B-08 2596_mmu_miR_130b	1.8275	0.79013142	7.6970E-02
02: N-11 2665_mmu_miR_200c	1.8395	0.19471432	4.3288E-03

Table 1, Continued.

03: B-21 2690_mmu_miR_375	1.93125	1.02005143	3.7137E-09
03: B-07 2718_mmu_miR_429	1.9365	0.15674502	3.3777E-12
01: N-11 2617_mmu_miR_26a	1.941	0.53461575	1.3319E-02
03: B-10 2592_mmu_let_7d	2.031	0.53468184	0.0000E+00
02: N-10 2547_mmu_miR_182	2.07175	0.48531802	0.0000E+00
04: F-24 2613_mmu_miR_20	2.205	0.56836197	3.3800E-01
02: N-04 2559_mmu_miR_194	2.286	1.46218489	1.2474E-01
02: B-21 2642_mmu_miR_148b	2.3685	1.16924548	1.8155E-01
03: F-04 2605_mmu_let_7a	2.369	0.8037989	3.2412E-10
03: N-04 2607_mmu_let_7c	2.38475	1.4718667	5.3165E-01
02: N-13 2661_mmu_miR_28	2.47475	0.84490369	3.2768E-03
03: J-04 2606_mmu_let_7b	2.48475	1.67906708	1.7760E-05
01: B-08 2500_mmu_let_7i	2.588	0.56351457	4.3108E-04
01: J-08 2502_mmu_miR_15b	2.63925	0.78334598	8.0270E-05
03: J-17 2700_mmu_miR_335	2.6865	0.53333823	6.0513E-01
02: F-10 2545_mmu_miR_129_5p	2.7125	0.55498258	2.2327E-05
02: N-15 2657_mmu_miR_17_5p	2.8285	0.91842819	2.6725E-01
02: J-08 2550_mmu_miR_185	2.85	0.88150591	4.3637E-02
01: B-06 2504_mmu_miR_27b	2.91975	0.83073878	2.4947E-06
03: B-02 2608_mmu_let_7e	2.948	1.18981091	2.7004E-05
01: N-08 2503_mmu_miR_23b	2.9505	0.92346215	1.0586E-03
03: F-02 2609_mmu_let_7f	2.96975	0.99896192	1.7399E-08
03: F-23 2687_mmu_miR_361	3.1125	0.36235296	2.6901E-01
01: J-05 2628_mmu_miR_98	3.22875	0.66773117	3.6208E-02
01: B-09 2618_mmu_miR_26b	3.28475	0.56195396	1.4403E-06
02: F-12 2541_mmu_miR_153	3.44675	1.5554805	0.0000E+00
02: F-15 2655_mmu_miR_107	3.45125	0.49530016	2.0375E-01
01: N-10 2499_mmu_let_7g	3.497	0.55032536	2.4624E-11
02: B-08 2548_mmu_miR_183	3.6905	0.72611684	4.8134E-04
01: N-07 2625_mmu_miR_96	4.29325	2.84800718	5.9887E-02
02: J-17 2652_mmu_miR_351	4.3265	1.61040626	2.0912E-02
01: N-09 2621_mmu_miR_27a	4.93375	5.12485098	0.0000E+00
01: J-11 2616_mmu_miR_23a	6.034	3.3033374	1.6554E-03
02: B-05 2674_mmu_miR_320	6.58275	5.94818383	6.5844E-04
02: B-03 2678_mmu_miR_222	7.09275	2.06657742	6.7703E-10
02: F-17 2651_mmu_miR_350	9.62025	2.74234284	6.0501E-02
02: J-22 2522_mmu_miR_132	**10.76825**	1.28805496	3.6079E-05
01: B-03 2630_mmu_miR_424	11.08425	2.41512476	6.8394E-05
02: N-14 2539_mmu_miR_151	20.84575	21.2696586	2.2624E-03
03: J-07	41.11525	40.6137845	4.8217E-02
02: F-09 2667_mmu_miR_212	**41.82925**	26.7431681	0.0000E+00
	median	1.82125	

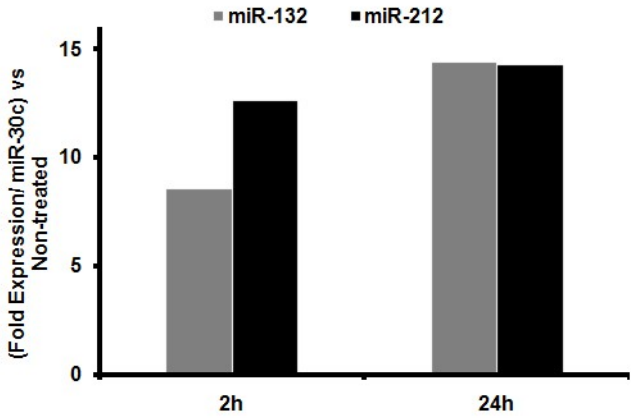

Figure 5. Verification by qPCR of miR-132/212 induction.
QPCR analysis using TaqMan micro-RNA Assays for mature miR-132 and miR-212 , which discriminates against pri- and pre-miRNAs (Ambion). Cells were treated with 10nM GnRH following 24 hours starvation. Data is fold expression of each miRNA normalized to non-treated cells. miR-30c was used as the internal control since microarray data showed expression did not change with GnRH treatment

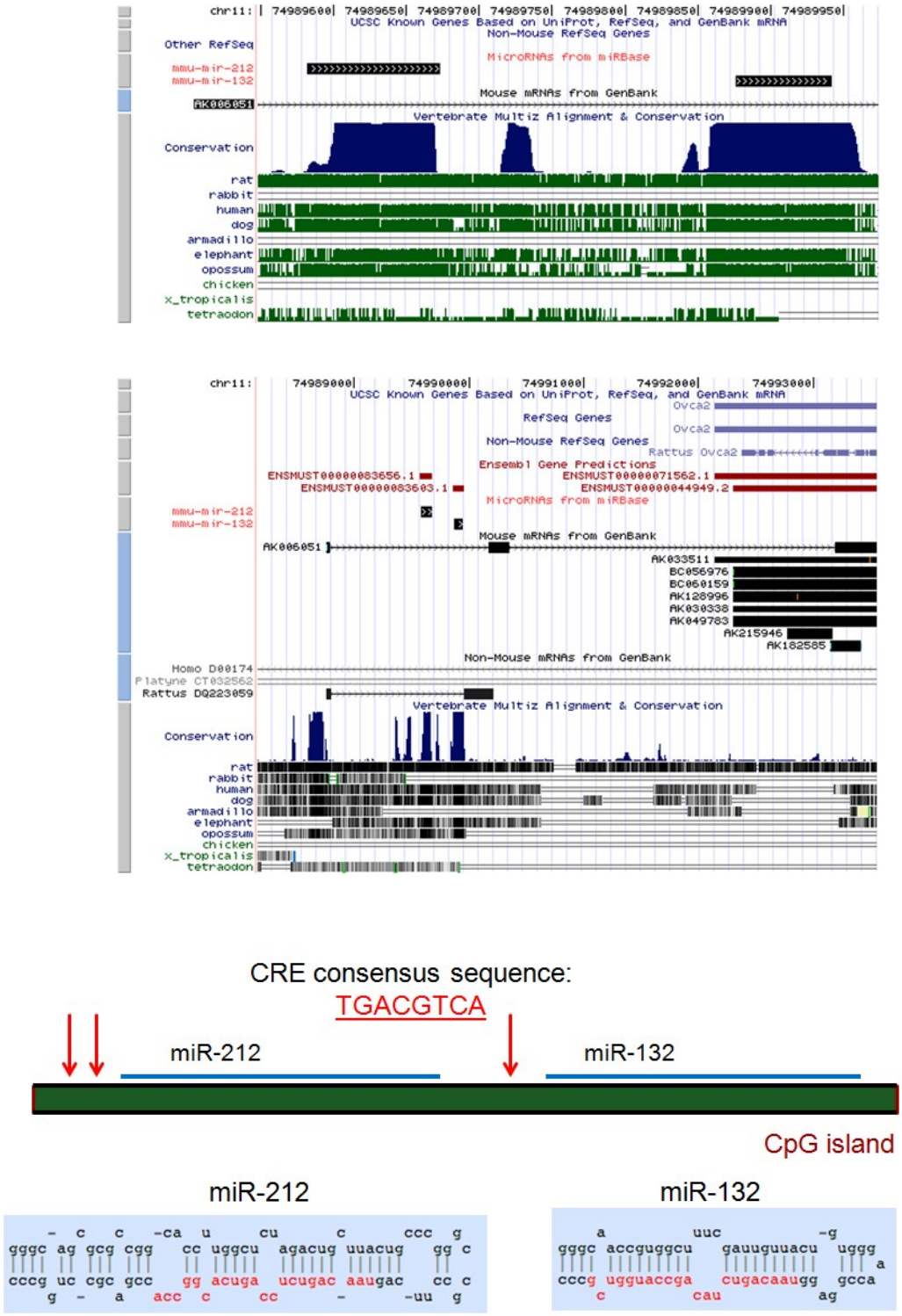

Figure 6. miR-132/212 are encoded in the same intron.
Schematic of the loci of miR-132/212 in mouse to the EST AK006051 and its conservation among various vertabrates. Both miR-132/212 have consensus CRE sites directly upstream.

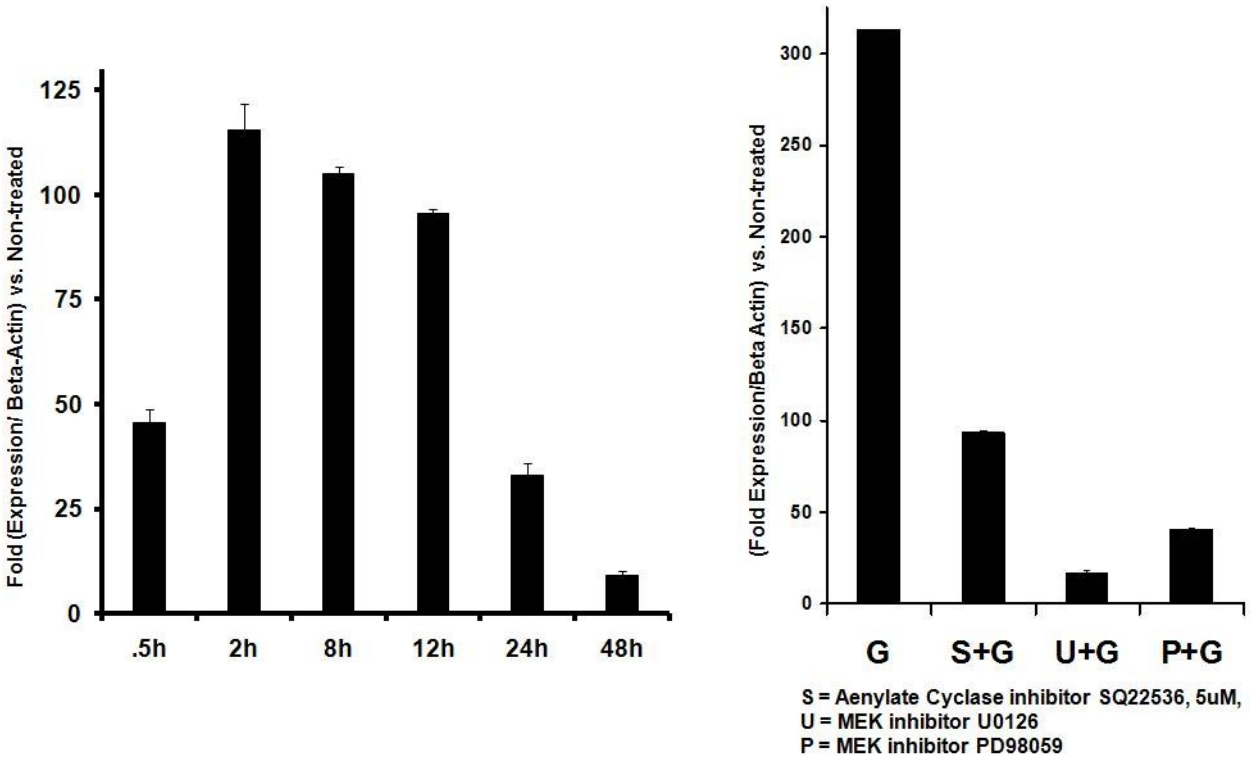

Figure 7. The non-coding mouse EST AK006051 is induced by GnRH via CREB and ERK.
QPCR analysis using primers flanking the first intron of AK006051. Cells were treated with 10nM GnRH following 24-hour starvation for the times shown. (left graph). To study signaling events upstream of AK006051 induction, cells were pretreated with AC or MEK inhibitors for 1 hour prior to 10nM GnRH stimulation.

A

AK006051: 1300nt Uptstream of Transcriptonal Start Site:

```
CACAGTTTCAAGTCTACGGCTAGCCTCGAACTCACAAAGGCGTCTACTTCCCACGTACAAGGA
TGCGCACCACCATGCCCCTCCTCTTAACTTTGCTTTCCCCTTCTTCCTGAGCTCCTCTGGTCA
TCCTGGTGCAGCTTCCTCCTCTCCGTGAACGCATGACGACCCCATTTAGAGCCCGGAGACAGA
ATCGGGCTGTTTTGGAGGACCTGTTCCATATCGTATTTGCCTTTAGTCTATTCTGACTCCTTT
AGAAAGGAGTCCCAGCTACACACACCCTCTGCCAAGCTATTGAGCCCCCTTAGTCTCATTTTC
TCTCTTACAGGCTCTGCCTATGCCTATTCCACCCCACTGAGGTGGCCCCCTCGTGCCCCCTGG
GGCACTGCCAAGTTGGCTCTCCAGTACTTGTCAGGCTAGCCCTTCCTTTTGTGGATACTCCGT
ACAGGGATTTTCCAAACTCTTACAGAAGATCTTCTGCTCATTTCTAAAGTCCAGACCACTCTC
CTTAGACTCCCTGATCTTCTCTGCGGTTTCCACCATCTGACCGGTACCTTTCCTCCTGTGACC
CAGTCAAGAAGCCTTCCAAAACTCCCAGGCTTCTCCACCCCTCTTTCCCAGCTCCTAGATGT
CAAAGTCCGAGGTGCACTCTACTCCCCTCCTAAACCGGTCCAGTTTCTTGCCTCACCCCCCAC
CCCCCCCCCACACACACCAGGAGAGAGCGAGGATACCACGGTGGCCAAATGGGAGTGATAC
CATCGCGGGGGCATCTTCTGGCGTCAGAGGACTGTAGGGTCTAGGGAATGAGCAGTGTGGTTG
GGGCTGCCAAGGGAGGACCCCTGCGGTCCAGGAGAAAAGAACTGAGATCCTAGGACTCGCAAA
GCCCCGGAAGGGGAGAGTGAATAAACACAGAACGGGGCCTCACCCTCCCTGCACTATTCTCCC
CCAGCCCGTCGCCTGCAGTTCCGGAAAGTTAACCCCTTGGAGGCCAAGCCTGGGGTTACGTAC
TCCCCTACCCAACCCTGCTTCCGCGTGCGCACCCTCCTCCCGCTCCAACTCCCTGTCGCTTCG
TCCCGCCCTCCCCTACGCCCCCCTCCCCGCTTGCCACTATAAATAGCCTCTTTTCCCGTTTC
CTAAATTCTCTGCTGACGTCGGCAGCGCGTCAGTGTGTAGGAGCCGCGGCCGCATGAATGAGC
CGCCGCACGAGTACTACGCGCGCCTATAAAGCGGCGGCGCCGGCCGGGCTGCGGGAGGCAAG
CCGGCACTGGTGCGACGCGGCCCGACAGGTAAGGACCACCAACAGTCGGAGATGGGCAGATGC
GCCGACGCCATGGGAAGGCGAGGAGGGGACCGGAGGGCGCGGCGGTTGGAGGGGGACTCCGGA
GTGAGGATGGGGGGCAGAGTGCGAGGGACGAAGGTTCCTTTCAGCTTGGTGGACCAGGGGCCG
GCGGCTGACCCAACCCTATGCAGCACCTGCCGGCACCCAAATGCAGACGCA
```

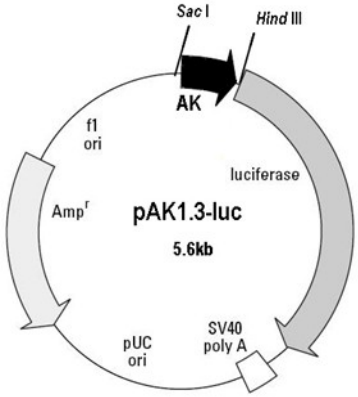

B

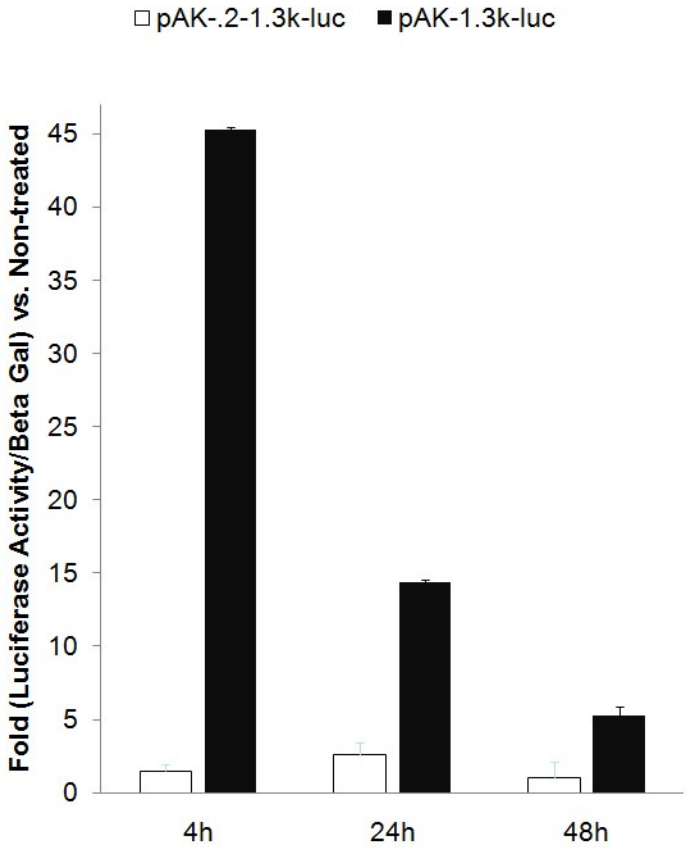

Figure 8. GnRH induces the AK006051 promoter Activity.
Luciferase activity of AK006051 promoter luciferase plasmid. (A) A luciferase vector (pAK-1.3-luc) was constructed by cloning 1.3kb upstream of the AK006051 transcriptional start site and inserting it into the promoter region of the luciferase plasmid pAP1-luc (Clontech) after the AP1 promoter was extracted by restriction digest. A control vector (pAK-.2-3) was also contructed using a truncated promoter region lacking the first 200bp upstream of the AK006051 transcriptional start site. (B) Cells were starved for 24 hours following transfection and treated with 10nM GnRH.

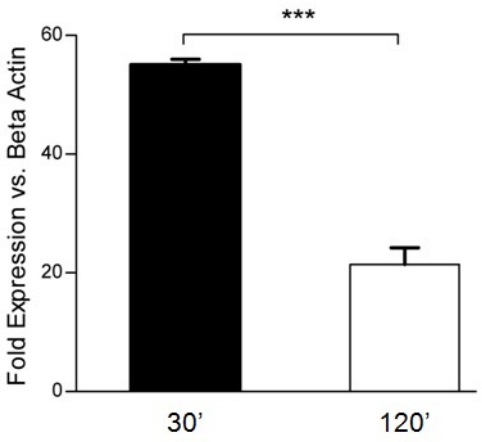

Figure 9. AK006051 expression is Sensitive to GnRH Pulse Frequency.
Cells were starved for 24 hours prior to beginning pulse treatments. For the duration of the experiment, media was changed every 30 minutes. For GnRH stimulation, media containing 10nM GnRH and 2ng/ml Activin was added to cells for 2 minutes at frequencies of 30 minutes or 120 minutes.

Table 2. Potential miR-132/212 Targets Predicted by MiRANDA

Species	Gene Name	Transcript	Description	GO Terms	Total Score	Total Energy	P value	Length	Total Sites	No. Cons Species	No. miRNAs
Mus musculus	Grit	ENSMUST00000047637	Rho GTPase-activating protein [Source:MarkerSymbol;Acc:MGI:2450166]		18.4036	-19.02	1.41005e-10	136	1	9	15 [+]
Mus musculus	Tjap1	ENSMUST00000087020	tight junction associated protein 1 [Source:MarkerSymbol;Acc:MGI:1921344]		18.5229	-23.3	9.42005e-10	542	1	6	54 [+]
Mus musculus	2310022A10Rik	ENSMUST00000067386	RIKEN cDNA 2310022A10 gene (2310022A10Rik), mRNA [Source:RefSeq_dna;Acc:NM_175107]		16.7488	-25.23	6.3567e-08	1257	2	7	23 [+]
Mus musculus	Alkbh3	ENSMUST00000040005	alkB, alkylation repair homolog 3 (E. coli) [Source:MarkerSymbol;Acc:MGI:1916363]		16.5746	-21.54	7.03196e-07	248	1	6	64 [+]
Mus musculus	Grm3	ENSMUST00000004076	glutamate receptor, metabotropic 3 [Source:MarkerSymbol;Acc:MGI:1351340]		16.5267	-15.23	8.83e-07	532	1	9	36 [+]
Mus musculus	Klhl11	ENSMUST00000056665	kelch-like 11 (Drosophila) [Source:MarkerSymbol;Acc:MGI:2388648]		17.3748	-19.4	1.64035e-06	252	2	7	59 [+]
Mus musculus	Paip2	ENSMUST00000041314	polyadenylate-binding protein-interacting protein 2 [Source:MarkerSymbol;Acc:MGI:1915119]		15.8843	-20.46	3.14837e-06	929	1	8	39 [+]
Mus musculus	TIM9_MOUSE	ENSMUST00000050130	Mitochondrial import inner membrane translocase subunit Tim9. [Source:Uniprot/SWISSPROT;Acc:Q9WV98]		17.4793	-14.82	3.4328e-06	379	1	8	52 [+]
Mus musculus	Pdia6	ENSMUST00000057288	protein disulfide isomerase associated 6 [Source:MarkerSymbol;Acc:MGI:1919103]		16.4204	-24.64	4.98048e-06	764	1	8	42 [+]
Mus musculus	Psmd13	ENSMUST00000026560	proteasome (prosome, macropain) 26S subunit, non-ATPase, 13 [Source:MarkerSymbol;Acc:MGI:1345192]		15.4816	-21.12	7.37394e-06	354	1	6	63 [+]
Mus musculus	Mcm2	ENSMUST00000058011	minichromosome maintenance deficient 2 mitotin (S. cerevisiae) [Source:MarkerSymbol;Acc:MGI:105380]		17.623	-21.06	1.36018e-05	524	1	8	48 [+]
Mus musculus	Sqle	ENSMUST00000022977	squalene epoxidase [Source:MarkerSymbol;Acc:MGI:109296]		15.0886	-12.07	1.51043e-05	275	1	6	58 [+]
Mus musculus	Slc25a20	ENSMUST00000035222	solute carrier family 25 (mitochondrial carnitine/acylcarnitine translocase), member 20		15.5583	-25.42	1.54453e-05	747	1	7	37 [+]

Table 3. miR-132/212 targets predicted by TargetScan

Number of conserved targets: 230
Number of conserved sites: 243

Human ortholog of target gene	Gene name	Conserved sites			
		total	8mer	7mer-m8	7mer-1A
NOVA1	neuro-oncological ventral antigen 1	2	1	0	1
SOX5	SRY (sex determining region Y)-box 5	2	1	0	1
OSBPL8	oxysterol binding protein-like 8	2	0	2	0
PRICKLE2	prickle-like 2 (Drosophila)	2	0	2	0
ARID2	AT rich interactive domain 2 (ARID, RFX-like)	2	0	1	1
BTBD7	BTB (POZ) domain containing 7	2	0	1	1
HMGA2	high mobility group AT-hook 2	2	0	1	1
SRGAP3	SLIT-ROBO Rho GTPase activating protein 3	2	0	1	1
TAF4	TAF4 RNA polymerase II, TATA box binding protein (TBP)-associated factor, 135kDa	2	0	1	1
ZNF238	zinc finger protein 238	2	0	1	1
CDC2L6	cell division cycle 2-like 6 (CDK8-like)	2	0	0	2
ST18	suppression of tumorigenicity 18 (breast carcinoma) (zinc finger protein)	2	0	0	2
STX16	syntaxin 16	2	0	0	2
BOLL	bol, boule-like (Drosophila)	1	1	0	0
BRWD1	bromodomain and WD repeat domain containing 1	1	1	0	0
C14orf43	chromosome 14 open reading frame 43	1	1	0	0
C5orf13	chromosome 5 open reading frame 13	1	1	0	0
C8orf13	chromosome 8 open reading frame 13	1	1	0	0
CALU	calumenin	1	1	0	0
CSDE1	cold shock domain containing E1, RNA-binding	1	1	0	0
DAZAP2	DAZ associated protein 2	1	1	0	0
DPYSL3	dihydropyrimidinase-like 3	1	1	0	0
DUSP9	dual specificity phosphatase 9	1	1	0	0
EP300	E1A binding protein p300	1	1	0	0
FLJ36888	hypothetical protein FLJ36888	1	1	0	0
FOXA1	forkhead box A1	1	1	0	0
FOXO3A	forkhead box O3A	1	1	0	0
KCNA6	potassium voltage-gated channel, shaker-related subfamily, member 6	1	1	0	0
LIN28B	lin-28 homolog B (C. elegans)	1	1	0	0
LRRFIP1	leucine rich repeat (in FLII) interacting protein 1	1	1	0	0
LSM11	LSM11, U7 small nuclear RNA associated	1	1	0	0
MAPK1	mitogen-activated protein kinase 1	1	1	0	0
MECP2	methyl CpG binding protein 2 (Rett syndrome)	1	1	0	0
MYCBP2	MYC binding protein 2	1	1	0	0
PAIP2	poly(A) binding protein interacting protein 2	1	1	0	0
PFN2	profilin 2	1	1	0	0
POM121	POM121 membrane glycoprotein (rat)	1	1	0	0
RKHD2	ring finger and KH domain containing 2	1	1	0	0
SEMA4G	sema domain, immunoglobulin domain (Ig), transmembrane domain (TM) and short cytoplasmic domain, (semaphorin) 4G	1	1	0	0
SPPL3	signal peptide peptidase 3	1	1	0	0
SPRED1	sprouty-related, EVH1 domain containing 1	1	1	0	0
SSH2	slingshot homolog 2 (Drosophila)	1	1	0	0
TIMM9	translocase of inner mitochondrial membrane 9 homolog (yeast)	1	1	0	0
TJAP1	tight junction associated protein 1 (peripheral)	1	1	0	0
USP9X	ubiquitin specific peptidase 9, X-linked	1	1	0	0

Table 3, Continued.

USP9Y	ubiquitin specific peptidase 9, Y-linked (fat facets-like, Drosophila)	1	1	0	0
ZFHX1B	zinc finger homeobox 1b	1	1	0	0
ADAMTS5	ADAM metallopeptidase with thrombospondin type 1 motif, 5 (aggrecanase-2)	1	0	1	0
ADCY3	adenylate cyclase 3	1	0	1	0
AMD1	adenosylmethionine decarboxylase 1	1	0	1	0
ANP32A	acidic (leucine-rich) nuclear phosphoprotein 32 family, member A	1	0	1	0
ARHGEF11	Rho guanine nucleotide exchange factor (GEF) 11	1	0	1	0
ATXN1	ataxin 1	1	0	1	0
BCAN	brevican	1	0	1	0
BCDIN3	bin3, bicoid-interacting 3, homolog (Drosophila)	1	0	1	0
BNC2	basonuclin 2	1	0	1	0
BNIP2	BCL2/adenovirus E1B 19kDa interacting protein 2	1	0	1	0
BRCA1	breast cancer 1, early onset	1	0	1	0
BRI3	brain protein I3	1	0	1	0
BTG2	BTG family, member 2	1	0	1	0
C14orf147	chromosome 14 open reading frame 147	1	0	1	0
C1QL1	complement component 1, q subcomponent-like 1	1	0	1	0
C1orf108	chromosome 1 open reading frame 108	1	0	1	0
C1orf121	chromosome 1 open reading frame 121	1	0	1	0
C6orf106	chromosome 6 open reading frame 106	1	0	1	0
CBX1	chromobox homolog 1 (HP1 beta homolog Drosophila)	1	0	1	0
CFL2	cofilin 2 (muscle)	1	0	1	0
CNIH	cornichon homolog (Drosophila)	1	0	1	0
CREB5	cAMP responsive element binding protein 5	1	0	1	0
DAG1	dystroglycan 1 (dystrophin-associated glycoprotein 1)	1	0	1	0
DEDD	death effector domain containing	1	0	1	0
DNAJA2	DnaJ (Hsp40) homolog, subfamily A, member 2	1	0	1	0
DNAJB14	DnaJ (Hsp40) homolog, subfamily B, member 14	1	0	1	0
EIF4A2	eukaryotic translation initiation factor 4A, isoform 2	1	0	1	0
FAM76B	family with sequence similarity 76, member B	1	0	1	0
FEM1C	fem-1 homolog c (C.elegans)	1	0	1	0
FKBP2	FK506 binding protein 2, 13kDa	1	0	1	0
FLJ45686	No Description	1	0	1	0
GTDC1	glycosyltransferase-like domain containing 1	1	0	1	0
H2AFZ	H2A histone family, member Z	1	0	1	0
H3F3B	H3 histone, family 3B (H3.3B)	1	0	1	0
HMG2L1	high-mobility group protein 2-like 1	1	0	1	0
HN1	hematological and neurological expressed 1	1	0	1	0
HNRPM	heterogeneous nuclear ribonucleoprotein M	1	0	1	0
HNRPU	heterogeneous nuclear ribonucleoprotein U (scaffold attachment factor A)	1	0	1	0
HSPC129	No Description	1	0	1	0
ISL1	ISL1 transcription factor, LIM/homeodomain, (islet-1)	1	0	1	0
KCNJ12	potassium inwardly-rectifying channel, subfamily J, member 12	1	0	1	0
KCNJ2	potassium inwardly-rectifying channel, subfamily J, member 2	1	0	1	0
KCNK2	potassium channel, subfamily K, member 2	1	0	1	0
KIAA0265	KIAA0265 protein	1	0	1	0
KIAA1904	KIAA1904 protein	1	0	1	0
LARGE	like-glycosyltransferase	1	0	1	0
LOC112476	No Description	1	0	1	0
MGC23401	No Description	1	0	1	0
MGC42367	similar to 2010300C02Rik protein	1	0	1	0
MMP16	matrix metallopeptidase 16 (membrane-inserted)	1	0	1	0
NCALD	neurocalcin delta	1	0	1	0
NDRG4	NDRG family member 4	1	0	1	0
NEIL2	nei like 2 (E. coli)	1	0	1	0

Table 3, Continued.

NFYA	nuclear transcription factor Y, alpha	1	0	1	0
NMNAT2	nicotinamide nucleotide adenylyltransferase 2	1	0	1	0
NR4A2	nuclear receptor subfamily 4, group A, member 2	1	0	1	0
OLFM1	olfactomedin 1	1	0	1	0
PAPOLA	poly(A) polymerase alpha	1	0	1	0
PCDH10	protocadherin 10	1	0	1	0
PCGF3	polycomb group ring finger 3	1	0	1	0
PEA15	phosphoprotein enriched in astrocytes 15	1	0	1	0
PFTK1	PFTAIRE protein kinase 1	1	0	1	0
PHF20L1	PHD finger protein 20-like 1	1	0	1	0
PLXND1	plexin D1	1	0	1	0
PNN	pinin, desmosome associated protein	1	0	1	0
PPM1G	protein phosphatase 1G (formerly 2C), magnesium-dependent, gamma isoform	1	0	1	0
PPP2R5C	protein phosphatase 2, regulatory subunit B (B56), gamma isoform	1	0	1	0
PRPF4B	PRP4 pre-mRNA processing factor 4 homolog B (yeast)	1	0	1	0
PSMD12	proteasome (prosome, macropain) 26S subunit, non-ATPase, 12	1	0	1	0
PTBP2	polypyrimidine tract binding protein 2	1	0	1	0
PURB	purine-rich element binding protein B	1	0	1	0
PXN	paxillin	1	0	1	0
ProSAPiP1	ProSAPiP1 protein	1	0	1	0
RAB15	RAB15, member RAS onocogene family	1	0	1	0
RASA1	RAS p21 protein activator (GTPase activating protein) 1	1	0	1	0
RDX	radixin	1	0	1	0
RICS	**Rho GTPase-activating protein**	1	0	1	0
RKHD3	ring finger and KH domain containing 3	1	0	1	0
SAP30L	No Description	1	0	1	0
SCN3A	sodium channel, voltage-gated, type III, alpha	1	0	1	0
SEMA6A	sema domain, transmembrane domain (TM), and cytoplasmic domain, (semaphorin) 6A	1	0	1	0
SEPHS1	selenophosphate synthetase 1	1	0	1	0
SIRT1	**sirtuin (silent mating type information regulation 2 homolog) 1 (S. cerevisiae)**	1	0	1	0
SLC30A6	solute carrier family 30 (zinc transporter), member 6	1	0	1	0
SLC6A1	solute carrier family 6 (neurotransmitter transporter, GABA), member 1	1	0	1	0
SOX11	SRY (sex determining region Y)-box 11	1	0	1	0
SOX4	SRY (sex determining region Y)-box 4	1	0	1	0
SPRY1	sprouty homolog 1, antagonist of FGF signaling (Drosophila)	1	0	1	0
TAF15	TAF15 RNA polymerase II, TATA box binding protein (TBP)-associated factor, 68kDa	1	0	1	0
TCF7L1	transcription factor 7-like 1 (T-cell specific, HMG-box)	1	0	1	0
TMEFF1	transmembrane protein with EGF-like and two follistatin-like domains 1	1	0	1	0
TRIM2	tripartite motif-containing 2	1	0	1	0
TSC22D3	TSC22 domain family, member 3	1	0	1	0
WHSC1L1	Wolf-Hirschhorn syndrome candidate 1-like 1	1	0	1	0
WT1	Wilms tumor 1	1	0	1	0
YWHAG	tyrosine 3-monooxygenase/tryptophan 5-monooxygenase activation protein, gamma polypeptide	1	0	1	0
ZCCHC11	zinc finger, CCHC domain containing 11	1	0	1	0
ZNF644	zinc finger protein 644	1	0	1	0
A2BP1	ataxin 2-binding protein 1	1	0	0	1
ACHE	acetylcholinesterase (Yt blood group)	1	0	0	1
ACSL4	acyl-CoA synthetase long-chain family member 4	1	0	0	1
ADAMTS6	ADAM metallopeptidase with thrombospondin type 1 motif, 6	1	0	0	1
AEBP2	AE binding protein 2	1	0	0	1
ARHGAP21	Rho GTPase activating protein 21	1	0	0	1

Table 3, Continued.

ARHGAP27	Rho GTPase activating protein 27	1	0	0	1
ARMC1	armadillo repeat containing 1	1	0	0	1
BICD2	bicaudal D homolog 2 (Drosophila)	1	0	0	1
BSN	bassoon (presynaptic cytomatrix protein)	1	0	0	1
C17orf42	chromosome 17 open reading frame 42	1	0	0	1
C18orf25	chromosome 18 open reading frame 25	1	0	0	1
CACNB4	calcium channel, voltage-dependent, beta 4 subunit	1	0	0	1
CBFA2T2	core-binding factor, runt domain, alpha subunit 2; translocated 2	1	0	0	1
CD164	CD164 antigen, sialomucin	1	0	0	1
CHES1	checkpoint suppressor 1	1	0	0	1
CITED2	Cbp/p300-interacting transactivator, with Glu/Asp-rich carboxy-terminal domain, 2	1	0	0	1
COLQ	collagen-like tail subunit (single strand of homotrimer) of asymmetric acetylcholinesterase	1	0	0	1
CPEB4	cytoplasmic polyadenylation element binding protein 4	1	0	0	1
DACH1	dachshund homolog 1 (Drosophila)	1	0	0	1
DNMT3A	DNA (cytosine-5-)-methyltransferase 3 alpha	1	0	0	1
EIF2C2	eukaryotic translation initiation factor 2C, 2	1	0	0	1
FLJ10357	hypothetical protein FLJ10357	1	0	0	1
FLJ22833	No Description	1	0	0	1
FLJ31818	hypothetical protein FLJ31818	1	0	0	1
FLJ45803	FLJ45803 protein	1	0	0	1
FMR1	fragile X mental retardation 1	1	0	0	1
FOXP1	forkhead box P1	1	0	0	1
FUSIP1	FUS interacting protein (serine/arginine-rich) 1	1	0	0	1
GATA2	GATA binding protein 2	1	0	0	1
GMFB	glia maturation factor, beta	1	0	0	1
GNA12	guanine nucleotide binding protein (G protein) alpha 12	1	0	0	1
GNB1	guanine nucleotide binding protein (G protein), beta polypeptide 1	1	0	0	1
HAO1	hydroxyacid oxidase (glycolate oxidase) 1	1	0	0	1
HBEGF	heparin-binding EGF-like growth factor	1	0	0	1
HIC2	hypermethylated in cancer 2	1	0	0	1
HNRPH1	heterogeneous nuclear ribonucleoprotein H1 (H)	1	0	0	1
HS2ST1	heparan sulfate 2-O-sulfotransferase 1	1	0	0	1
ITGA9	integrin, alpha 9	1	0	0	1
ITPKB	inositol 1,4,5-trisphosphate 3-kinase B	1	0	0	1
KIAA0240	KIAA0240	1	0	0	1
LASS2	LAG1 longevity assurance homolog 2 (S. cerevisiae)	1	0	0	1
LIN9	lin-9 homolog (C. elegans)	1	0	0	1
LOC401498	similar to RIKEN A930001M12	1	0	0	1
LOC93081	No Description	1	0	0	1
MEGF11	MEGF11 protein	1	0	0	1
MEIS1	Meis1, myeloid ecotropic viral integration site 1 homolog (mouse)	1	0	0	1
MGC17330	HGFL gene	1	0	0	1
MGC48972	No Description	1	0	0	1
MYST2	MYST histone acetyltransferase 2	1	0	0	1
NET1	neuroepithelial cell transforming gene 1	1	0	0	1
NFAT5	nuclear factor of activated T-cells 5, tonicity-responsive	1	0	0	1
NLK	nemo-like kinase	1	0	0	1
OSBPL11	oxysterol binding protein-like 11	1	0	0	1
PDE7B	phosphodiesterase 7B	1	0	0	1
PLAGL2	pleiomorphic adenoma gene-like 2	1	0	0	1
PPP1R12A	protein phosphatase 1, regulatory (inhibitor) subunit 12A	1	0	0	1
PRKD1	protein kinase D1	1	0	0	1
PSMA2	proteasome (prosome, macropain) subunit, alpha type, 2	1	0	0	1
PTCH	patched homolog (Drosophila)	1	0	0	1
QKI	quaking homolog, KH domain RNA binding (mouse)	1	0	0	1

Table 3, Continued.

RAB28	RAB28, member RAS oncogene family	1	0	0	1
RAB6B	RAB6B, member RAS oncogene family	1	0	0	1
RTN4	reticulon 4	1	0	0	1
SATB2	SATB family member 2	1	0	0	1
SFRS1	splicing factor, arginine/serine-rich 1 (splicing factor 2, alternate splicing factor)	1	0	0	1
SOX2	SRY (sex determining region Y)-box 2	1	0	0	1
TCEB1	transcription elongation factor B (SIII), polypeptide 1 (15kDa, elongin C)	1	0	0	1
TCF7L2	transcription factor 7-like 2 (T-cell specific, HMG-box)	1	0	0	1
TLN2	talin 2	1	0	0	1
TLOC1	translocation protein 1	1	0	0	1
TMEM2	transmembrane protein 2	1	0	0	1
TRIB2	tribbles homolog 2 (Drosophila)	1	0	0	1
UBE2D3	ubiquitin-conjugating enzyme E2D 3 (UBC4/5 homolog, yeast)	1	0	0	1
USP15	ubiquitin specific peptidase 15	1	0	0	1
USP6	ubiquitin specific peptidase 6 (Tre-2 oncogene)	1	0	0	1
VAPA	VAMP (vesicle-associated membrane protein)-associated protein A, 33kDa	1	0	0	1
VDAC2	voltage-dependent anion channel 2	1	0	0	1
WDR42A	WD repeat domain 42A	1	0	0	1
ZFYVE1	zinc finger, FYVE domain containing 1	1	0	0	1
ZHX1	zinc fingers and homeoboxes 1	1	0	0	1
ZNF207	zinc finger protein 207	1	0	0	1
ZNF365	zinc finger protein 365	1	0	0	1
ZNF395	zinc finger protein 395	1	0	0	1
ZNF650	zinc finger protein 650	1	0	0	1

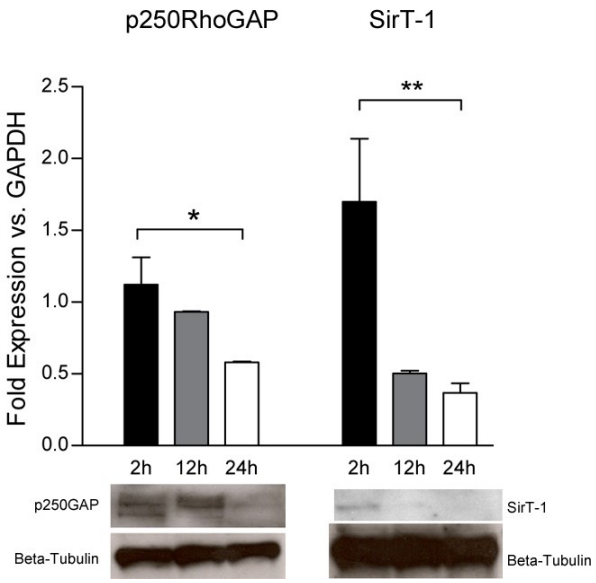

Figure 10. GnRH reduces p250RhoGAP and SirT-1.
Cells were treated with 10nM GnRH after 24 hours starvation. QPCR analysis of p250RhoGAP and SirT-1 mRNA fold expression normalized to non-treated cells. B. Protein levels of p250RhoGAP and SirT-1.

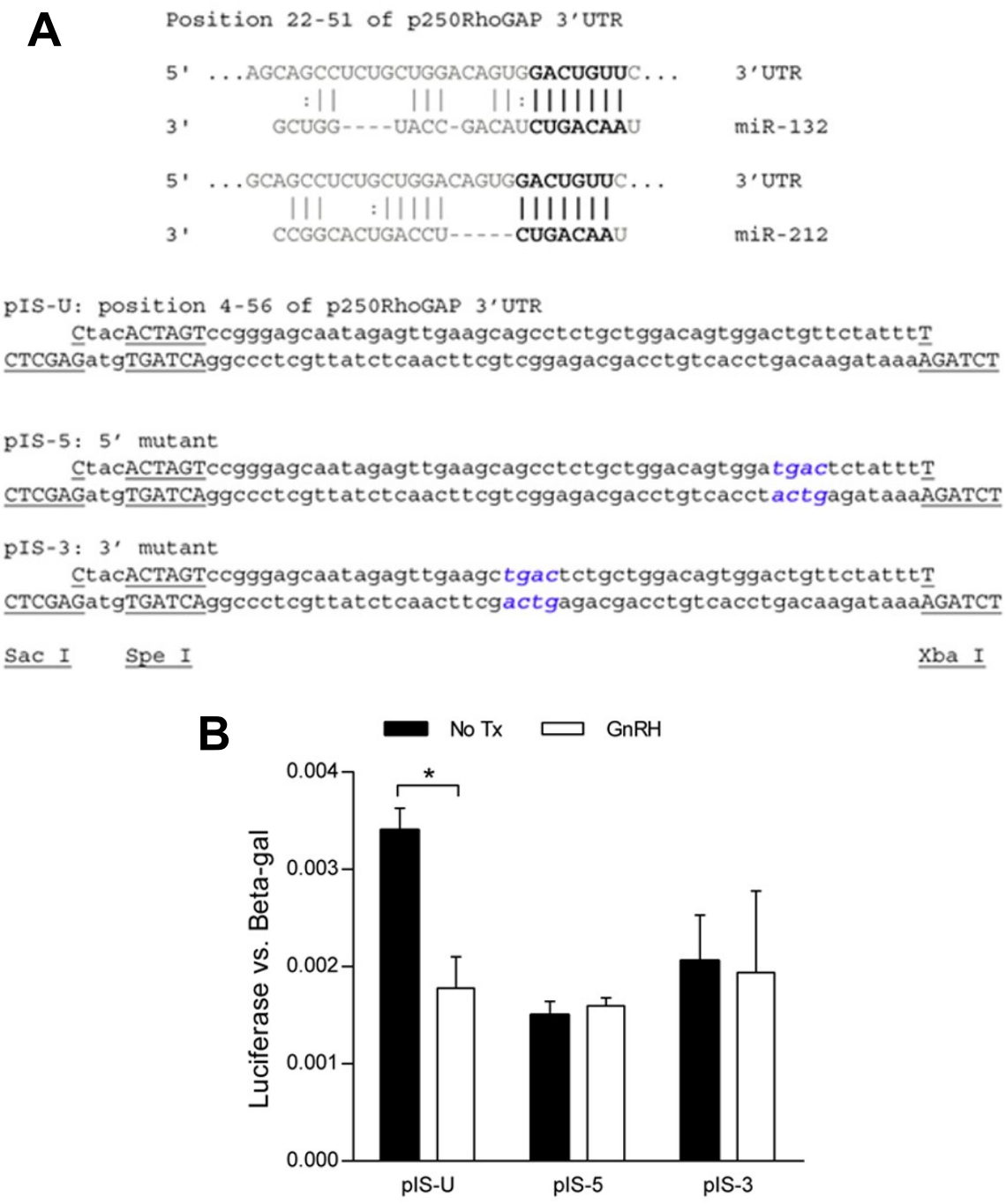

Figure 11. The MRE of p250RhoGAP confers suppression of luciferase mRNA.
(A)Luciferase reporters were constructed by inserting the 3'UTR region of p250RhoGAP containing the recognition sequence for miR-132/212 into the MCS of the pIS luciferase vector (pIS-U). Two mutants were also constructed in which the UTR region complementary to either the 5' or 3' region of miR-132/212. Inserts were constructed by Klenow fill-in with Sac I, Spe I, and Xba I restriction sites. (B) Luciferase activity of pIS reporter constructs. Twenty-four hours after co-transfection with tk-lacZ plasmid, cells were starved for 24 hours before treatment with 10nM GnRH for 24 hours. Data is Luciferase activity normalized to beta-galactosidase activity

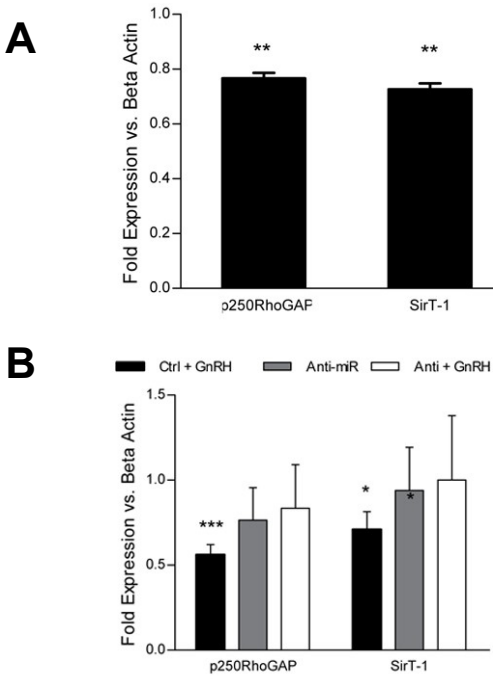

Figure 12. miR-132/212 target p250RhoGAP and SirT-1 for degradation.
(A) Pre-miR-132 reduces p250RhoGAP, SirT-1. QPCR analysis of miR-132/212 targets 48 hours following transfection of either Pre-miR-132 or control pre-miR (scrambled RNA hairpin) (Ambion). Data is fold expression normalized to non-treated cells. (B) Cells were transfected with anti-miR132/212 or scrambled control and harvested after 48 hours..

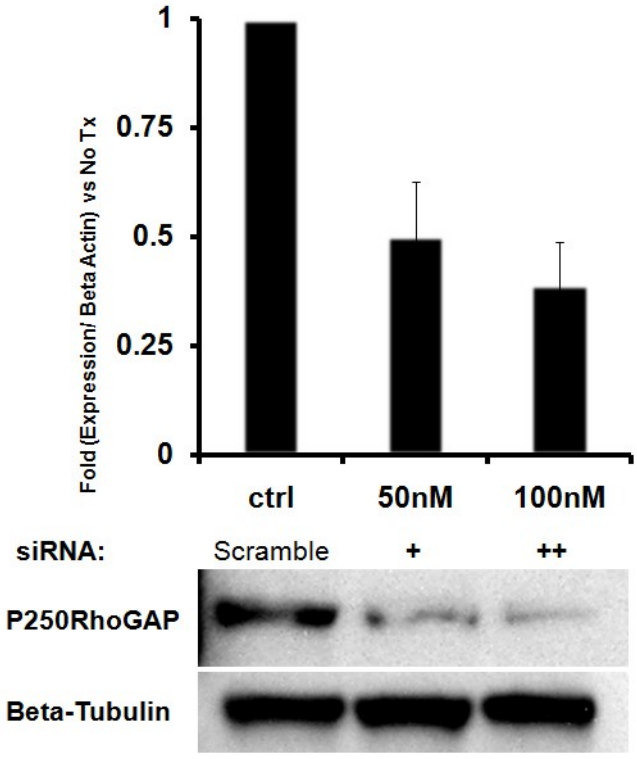

Figure 13. siRNA knockdown of p250RhoGAP.
Cells were transfected with siRNA against p250RhoGAP and harvested 48 hours later.

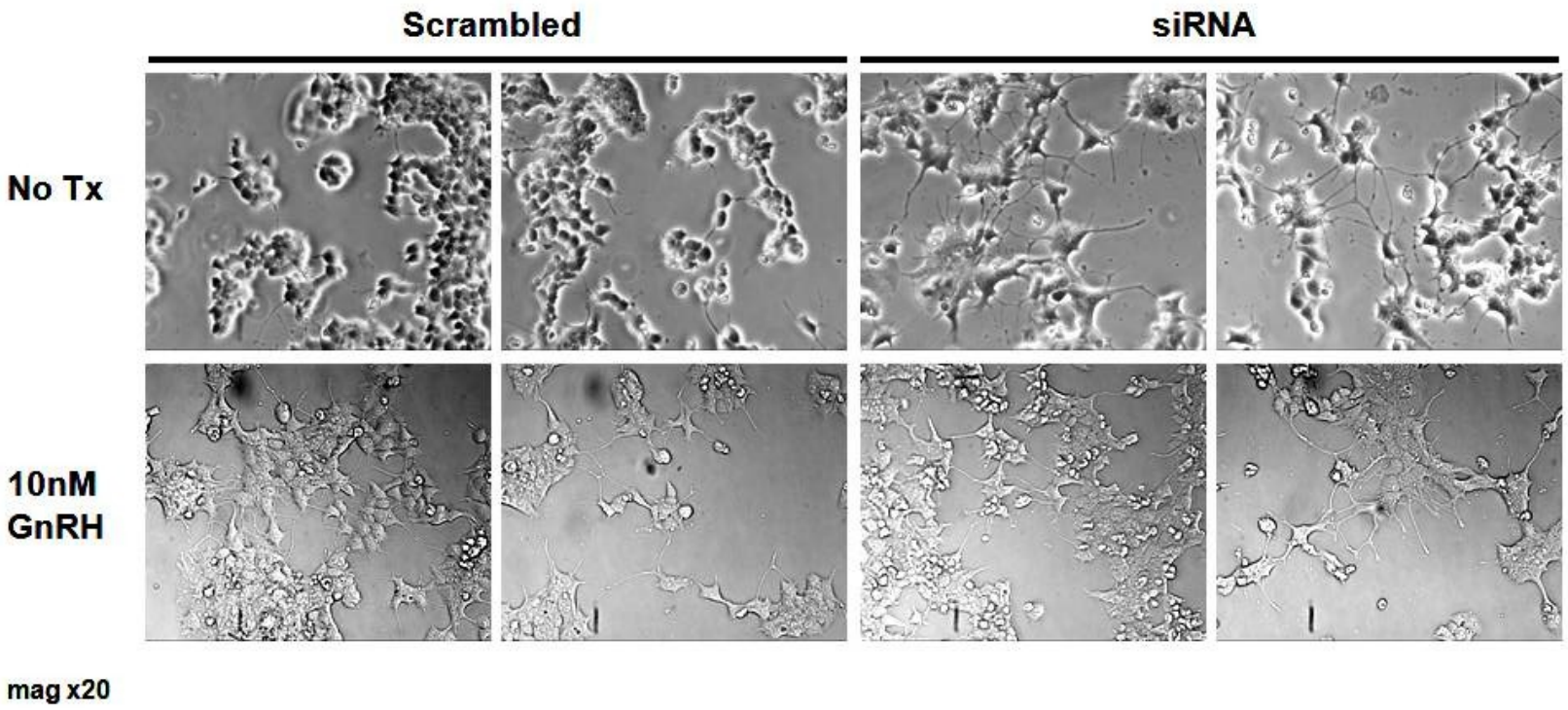

Figure 14. Knockdown of p250RhoGAP induces elaborate neurite outgrowth.
Cells were transfected with 100nM siRNA and cultured on poly-L-lysine- and Matrigel- coated plates for 24 hours followed by starvation for an additional 48 hours (Top row). Cells were then treated with 10nM GnRH for 24 hours.

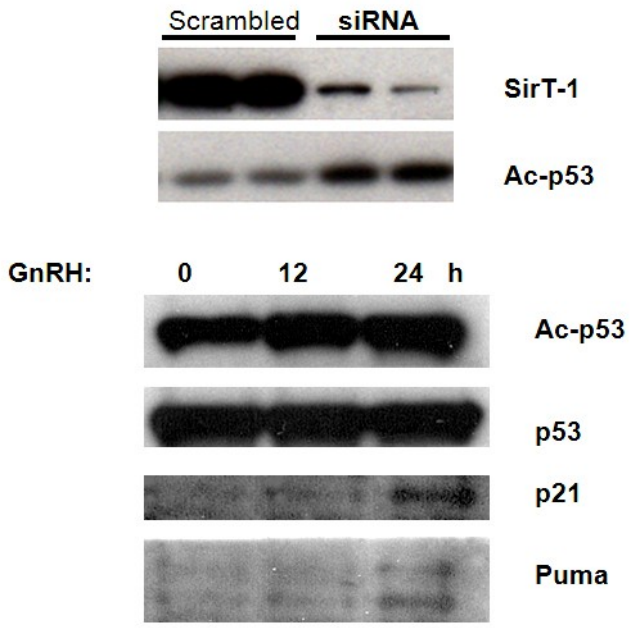

Figure 15. SirT-1 deacetylates p53 and prevents apoptosis. (Top) SirT-1 was knocked down by siRNA at a concentration of 5μM resulting in acetylation of p53. Blot was done by Debin Lan. (Bottom) GnRH increases p53 acetylation and induces p21 and Puma.

REFERENCES

1. Conn PM, Crowley Jr WF 1994 Gonadotropin-releasing Hormones and its analogs. Annu Rev Med 45:391-405

2. Kaiser UB, Conn PM, Chin WW 1997 Studies of gonadotropin-releasing homone (GnRH) action using GnRH receptor-expressing pituitary cell line. Endocr Rev 18:46-70

3. Liu F, Usui I, Evans LG, Austin DA, Mellon PL, Olefsky JM, Webster NJG 2002. Involvement of both Gq/11 and Gs proteins in gonadotropoin-releasing hormone receptor-mediated signaling in LßT2 Cells. JBC 277(35) 32099-32108

4. Shacham S, Cheifetz MN, Lewy H, Ashkenazi IE, Becker OM, Seger R. 1999. Mechanism of GnRH receptor signaling: from the membrane to the nucleus. Ann d'endo. 60(2):79-88.

5. Song SB, Rhee M., Roberson MS, Maurer RA, Kim KE. 2003. Gonadotropin-releasing hormone-induced stimulation of the rat secretogranin II promoter involves activation of CREB. Mol Cell Endo. 199 (1-2), pp. 29-36.

6. Ando H, Hew CL, Urano A. 2001. Signal transduction pathways and transcription factors involved in the gonadotropin-releasing hormone-stimulated gonadotropin subunit gene expression. Comparative Biochemistry and Physiology - B Biochemistry and Molecular Biology, 129 (2-3), pp. 525-532.

7. Gonzalez GA, Montminy MR. 1989. Cyclic AMP stimulates somatostatin gene transcription by phosphorylation of CREB at serine 133. Cell, 59 (4), pp. 675-680.

8. Lonze, BE, Ginty DD. 2002. Function and regulation of CREB family transcription factors in the nervous system Neuron, 35 (4): 605-623.

9. Stanislaus D, Janovick JA, Brothers S, Conn PM 1997 Regulation of G(q/11)α by the gonadotropin-releasing hormone receptor. Mol Endo 11:738–746

10. Liu F, Austin DA, Mellon PL, Olefsky JM, Webster JNG. 2002. GnRH Activates ERK1/2 Leading to the Induction of c-fos and LHß Protein Expression in LßT2 Cells. Mol Endo 16: 419 - 434.

11. Knobil E 1974. On the control of gonadotropin secretion in the rhesus monkey. Recent Prog rom Res 30:1-46

12. Turgeon JL, Windle JJ, Whyte DB, Mellon PL. 1994. GnRH and estrogen regulate secretion of LH from an immortal gonadotrope cell line. Program of the 76th Annual Meeting of the Endocrine Society, Anaheim, CA (Abstract 1781)

13. McGarvey C, Cates PA, Brooks A, Swanson IA, Milligan SR, Coen CW, O'Byrne KT. 2001. Phytoestrogens and gonadotropin-releasing hormone pulse generator activity and pituitary luteinizing hormone release in the rat. Endo 142:1202-1208

14. Zhang H, Bailey JS, Coss D, Lin B, Tsutsumi R, Lawson MA, Mellon PL, Webster NJG 2006 Activin Modulates the Transcriptional Response of LßT2 Cells to gonadotropin-releasing hormones and alters Cellular Proliferation. Mol Endo 20(11):2909-2930

15. Shacham S, Harris D, Ben-Shlomo H, Cohen I, Bonfil D, Przedecki F, Lewy H, Ashkenazi IE, Seger R, Naor Z. 2001. Mechanism of GnRH receptor signaling on gonadotropin release and gene expression in pituitary gonadotrophs. Vitam. Horm. 63: 63-90.

16. Navratil AM, Knoll JG, Whitesell JD, Tobet SA, Clay CM. 2007. Neuroendocrine plasticity in the anterior pituitary: gonadotropin-releasing hormone-mediated movement in vitro and in vivo. Endo 148(4):1736-1744

17. Bartel DP. 2004. MicroRNAs: genomics, biogenesis, mechanism, and function. Cell 116:281-297.

18. Lee Y, Kim M, Han J, Yeom KH, Lee S, Baek SH, Kim VN. 2004. MicroRNA genes aretranscribed by RNA polymerase II. Embo J 23: 4051-4060.

19. Lee Y, Jeon K, Lee JT, Kim S, Kim VN. 2002 MicroRNA maturation: stepwise processing and subcellular localization. Embo J 21: 4663-4670.

20. Kim VN. 2004 MicroRNA precursors in motion: exportin-5 mediates their nuclear export. TrendsCell Biol 14: 156-159.

21. Yi R, Qin Y, Macara IG, Cullen BR. 2003. Exportin-5 mediates the nuclear export of premicroRNAs and short hairpin RNAs. Genes Dev 17: 3011-3016.

22. Lewis BP, Shih IH, Jones-Rhoades MW, Bartel DP, Burge CB. 2003. Prediction of mammalian microRNA targets. Cell 115: 787-798.

23. Hutvagner G, Simard MJ. 2008. Argonaute proteins: key players in RNA silencing. Nat Rev Mol Cell Biol; 9: 22-32.

24. Lewis BP, Burge CB, Bartel DP. 2005. Conserved seed pairing, often flanked by adenosines, indicates that thousands of humangenes are microRNA targets. Cell 120, 15–20.

25. Grimson A., Farh KK-HK., Johnston WKK., Garrett-Engele P, Lim LPP, Bartel DP. 2007. Microrna targeting specificity in mammals: Determinants beyond seed pairing. Mol Cell 27(1): 91-105.

26. Bartel DP. 2004 MicroRNAs: genomics, biogenesis, mechanism, and function. Cell 116: 281-297.

27. Wienholds E, Plasterk RH. MicroRNA function in animal development. FEBS Lett 2005; 579: 5911-5922.

28. Hiroi H, Christenson LK, Chang L, Sammel MD, Berger SL, Strauss JF, 3rd. 2004. Temporal and spatial changes in transcription factor binding and histone modifications at the steroidogenic acute regulatory protein (stAR) locus associated with stAR transcription. Mol Endo 18: 791-806.

29. Yuen T, Ruf F, Chu T, Sealfon SC 2009 Microtranscriptome regulation by gonadotropin-releasing hormone Mol Cell Endo 302(1):12-17.

30. Edga D, Timpl. R, Thoenen, H. 1984. Mapping of domains in human laminin using monoclonal antibodies: localization of the neurite-promoting site. EMBO J., 3: 1463-1468.

31. Engvall E, Davis CE, Dickerson K, Ruoslahti R, Varon S, Manthorpe M. 1986. Mapping of domains in human laminin using monoclonal antibodies: localization of the neurite-promoting site. J Cell Bio 103:2457-2465.

32. Evercooren, B, Kleinman HK, Ohno, Marangos P, Schwartz JP, Dubois-Dalcq ME. 1982. Nerve growth factor, laminin and fibronectin promote neurite growth in human fetal sensory ganglion cultures. J. Neuro Res., 8: 179-193.

33. Hatten ME, Furie MB, Rifkin DB. 1982 Binding of developing mouse cerebellar cells to fibronectin: a possible mechanism for the formation of the external granular layer. J. Neuro 2: 1 1 95- 1 206.

34. Manthorpe M, Engvall E, Ruoslahti E, Longo FM, Davis GE, Varon S. 1983. Laminin promotes neurite regeneration from cultured peripheral and central neurons. J. cell Biol., 97: 1882-1898.

35. Rogers LR, Letourneau Pc, Palm SL, Mccarthy J, Furcht LT. 1983 Neurite extension by peripheral and central nervous system neurons in response to substratum-bound uibronectin and laminin. Dev. Biol., 98: 212-220.

36. Tomaselli KJ, Damsky CH, Reichardt LF. 1988 Purification and characterization of mammalian integrins expressed by a rat neuronal cell line (Pc12): evidence that they function as a/ı heterodimeric receptors for laminin and type lv collagen. J. Cell Bio, 107: 1241-1252.

37. Horacek MJ, Dada MO, Terracio L 1992. Reconstituted basement membrane influences prolactin, LH, and FSH secretion from adult and fetal adenohypophyseal cells in vitro. J Cell Physio 151:180-189.

38. Roelle S, Grosse R, Aigner A, Krell HW, Czubayko F, Gudermann T 2003 Matrix metalloproteinases 2 and 9 mediate epidermal growth factor receptor transactivation by gonadotropin-releasing hormone. J Biol Chem 78:47307-47318.

39. Vo N, Klein M, Varlamova O, Keller DM, Yamamoto T, Goodman RH, Impey S. 2005. A cAMP-response element binding protein-induced microRNA regulates neuronal morphogenesis. PNAS 102(45): 16426-16431.

40. Van Aeist L, Souza-Schorey CD. 1997 Rho GTPases and signaling networks. Genes Dev 11: 2295-2322.

41. Bishop AL, Hall A. 2000. Rho GTPases and their effector proteins. Biochem J 348: 241–255.

42. Sah VP, Seasholtz TM, Sagi SA, Brown JH. 2000. The role of Rho in G protein-coupled receptor signal transduction, Annu. Rev. Pharmacol. Toxicol. 40: 459–489.

43. Takai Y, Sasaki T, Matozaki T. 2001. Small GTP-binding proteins, Physiol. Rev. 81:153–208.

44. Shang X, Moon SY, Zheng Y. 2007. P200 RhoGAP promotes cell proliferation by mediating cross-talk between Ras and Rho signaling pathways. J Biol Chem 282(12): 8801-8811.

45. Imai S, Armstrong CM, Kaeberlein M, Guarente L. 2000. Transcriptional silencing and longevity protein Sir2 is an NAD-dependent histone deacetylase. Nature. 403: 795-800.

46. Kennedy BK, Smith ED, Kaeberlein M. 2005. The enigmatic role of Sir2 in aging. Cell. 18: 548-550.

47. Vaziri H, Dessain SK, Eaton N, Imai SI, Frye RA, Pandita TK, Guarente L, Weinberg RA. 2001. hSIR2(SIRT1) functions as an NAD-dependent p53 deacetylase. 2001. 107(2):149-159.

48. Wayman GAA., Davare M, Ando H, Fortin D, Varlamova O, Cheng H-Y MY, Marks D, Obrietan K., Soderling TRR, Goodman RHH, Impey S. 2008. An activity-regulated microrna controls dendritic plasticity by down-regulating p250gap. PNAS 105(26): 9093-9098.

49. Yamakuchi M, Ferlito M, Lowenstein CJ. 2008. mir-34a repression of sirt1 regulates apoptosis. PNAS 105(36):13421-13426.

50. Yamakuchi, M. and Lowenstein, C. J. 2009. Mir-34, sirt1 and p53: The feedback loop. Cell cycle (Georgetown, Tex.) 8.

51. Yekta S, Shih IH, Bartel DP. 2004. MicroRNA-directed cleavage of HOXB8 mRNA. Science. 304(5670):594-596.

52. Vogelstein B, lane D, Levine AJ. 2000. Surging the p53 network. Nature. 408:307-310.

53. Vogelstein G, Kinzler K. 2004. Cancer genes and the pathways they control. Nat Med 10:789-799.

54. Li M, Luo J, Brooks CL, Gu W. 2002. Acetylation of p53 inhibits its ubiquitination by Mdm2. JBC 277(52):50607-50611.

55. Zhao Y, Lu S, Wu L, Chai G, Wang H, Chen Y, Sun J, Yu Y, Zhou W, Zheng Q, Wu M, Otterson G, Zhu WG. 2006. Acetylation of p53 at Lysine 373/382 by the Histone Deacetylase Inhibitor Depsipeptide Induces Expression of p21Waf1/Cip1 Mol. Cell. Biol. 26(7): 2782-2790.

56. Coussens M, Maresh JG, Yanagimachi R, Maeda G, Allsopp R. 2008. SirT-1 deficiency attenuates spermatogenesis in germ cell function. PLoS ONE 3(2):e1571.

57. Li H, Rajendran GK, Liu N, Ware C, Rubin B, Gu Y. 2007. SirT1 modulates the estrogen-insulin-like growth factor-1 signaling for postnatal development of mammary gland in mice. Breast Can Res 9: R1.

58. Fiedler SD, Carletti MZ, Hong X, Christenson LK. 2008. Hormonal Regulation of MicroRNA Expression in Periovulatory Mouse Mural Granulosa Cells. Biol Reprod 79: 1030 – 1037.

59. Okabe T, Nakamura T, Nishimura YN, Kohu K, Ohwada S, Morishita Y, Akiyama T. 2003. RICS, a Novel GTPase-activating Protein for Cdc42 and Rac1, is involved in the β-catenin-N-cadherin and N-methyl-D-aspartate receptor signaling. JBC 278(11):9920-9927

60. Luo L, Hensch TK, Ackerman L, Barbel S, Jan LY, Jan YN. 1996. Differential effects of the Rac GTPase on perkinje cell axons and dendritic trunks and spines. Nature 379(6568): 837-840

61. Ziv NE, Smith SJ. 1996. Evidence for a role of dendritic filopodia in synaptogenesis and spine formation. Neuron 17(1): 91-102

62. Benarroch EE.. 2007. Rho GTPases. Neuro 68:1315-1318.

63. Da Silva JS, Schubert V, Dotti CG. 2004 RhoA, Rac1, and Cdc42 intracellular distribution shift during hippocampal neuron development. Mol Cell Neuro 27(1): 1-7.

64. Newey SE, Velamoor V, Govek EE, Van Aelst L. 2005. Rho GTPases, dendritic structure, and mental retardation. J Neurobiol 64:58–74.

65. Segal M. 2005 Dendritic spines and long-term plasticity. Nat Rev Neurosci 6:277–284.